

# Shipboard Condition Based Maintenance and Integrated Power System Initiatives

By

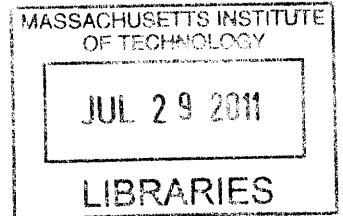
**Darrin E. Barber**

B.S., Electrical Engineering  
Prairie View A&M University, 2002

Submitted to the Department of Mechanical Engineering and the Department of Electrical Engineering and Computer Science in Partial Fulfillment of the Requirements for the Degrees of

Engineer in Naval Architecture and Marine Engineering  
and  
Master of Science in Electrical Engineering and Computer Science  
at the  
Massachusetts Institute of Technology  
June 2011

**ARCHIVES**



© 2011 Massachusetts Institute of Technology  
All rights reserved.

Signature of Author \_\_\_\_\_

*D*  
Darrin E. Barber  
Center for Ocean Engineering, Department of Mechanical Engineering  
May 6, 2011

Certified by \_\_\_\_\_

*S*  
Steven B. Leeb  
Professor of Electrical Engineering and Computer Science & Mechanical Engineering Department  
Thesis Advisor

Accepted by \_\_\_\_\_

*L*  
Leslie A. Kolodziejski  
Chairman, Department Committee on Graduate Students  
MIT Department of Electrical Engineering and Computer Science

Accepted by \_\_\_\_\_

*D*  
David E. Hardt  
Chairman, Department Committee on Graduate Students  
Department of Mechanical Engineering

(This Page Intentionally Left Blank)

# **Shipboard Condition Based Maintenance and Integrated Power System Initiatives**

By

Darrin E. Barber

B.S., Electrical Engineering  
Prairie View A&M University, 2002

Submitted to the Department of Mechanical Engineering and the Department of Electrical Engineering and Computer Science in Partial Fulfillment of the Requirements for the Degrees of

Engineer in Naval Architecture and Marine Engineering  
and  
Master of Science in Electrical Engineering and Computer Science

## **ABSTRACT**

With the U.S. Navy's continued focus on developing and implementing a robust integrated power system aboard future combatants, there has been an ever increasing effort to guarantee an electrical distribution system that maintains maximum capabilities in the event of a system fault. It is believed that the implementation of a device such as a non-intrusive load monitor (NILM) can greatly assist in the preemptive detection of such faults and failures.

Ongoing NILM research conducted at Massachusetts Institute of Technology's Laboratory for Electromagnetic and Electronic Systems (LEES) is exploring the application of NILM technology in shipboard environments. The NILM's unique ability to monitor the power usage profile of these systems can be used to immediately diagnose system casualties and unusual operation parameters. Additionally, research has shown that the NILM can be used effectively and reliably, to monitor equipment health, recognize and indicate abnormal operating conditions and casualties and provide invaluable information for training operators, diagnosing problems and troubleshooting.

This thesis will discuss how this frequency content of the aggregate measurement can be used to assess the health of motors. Experiments were conducted in the confines of LESS in addition to aboard USCGC ESCANABA (WMEC-907), a 270-foot Coast Guard Cutter, in order to better understand the system dynamics in a real life environment.

To further support the US Navy's integrated power system initiatives two hardware models of a shipboard electrical propulsion drive system were constructed, an MVDC propulsion simulation and a doubly-fed machine propulsion model. These simulations were built for the purpose of testing innovative integrated propulsion system theories, algorithms, configurations and new electric propulsion concepts.

Thesis Advisor: Steven B. Leeb

Title: Associate Professor of Electrical Engineering and Computer Science

(This Page Intentionally Left Blank)

## Acknowledgments

The author would like to acknowledge the following individuals for their assistance. Without them this thesis would not have been possible.

- Steven Leeb for providing me with a rewarding and challenging experience. This experience has been by far the most challenging and most rewarding of my academic career.
- Jim Paris for providing his expertise when any software issues arose.
- Warit Wichakool for providing insight on the aspects of conducting experiments and ensuring that they were conducted safely within the lab and in the field.
- Uzoma Orji for his software and technical expertise and willingness to help on a daily basis with any issues that arose.
- Chris Schantz for his mechanical expertise, willingness to help and crafty ability to discover simple solutions to complex problems.
- Andy Carlston for his expertise in designing and constructing many of the platforms required for experiments.
- LT Andrew Goshorn and LTjg Kevin Thomas for all the support they provided during the experiments aboard the *USCGC ESCANABA (WMEC-907)*.

To my parents, Thomas and Deborah Barber and fiancé, Delicia Wiles, for always being by my side and providing support throughout this entire process.

(This Page Intentionally Left Blank)

# Table of Contents

<b>ABSTRACT .....</b>	<b>3</b>
<b>CHAPTER 1: INTRODUCTION .....</b>	<b>13</b>
<b>1.1 BACKGROUND .....</b>	<b>13</b>
<b>1.2 U.S. COAST GUARD INITIATIVES .....</b>	<b>15</b>
<b>1.3 U.S. NAVY INITIATIVES .....</b>	<b>15</b>
<b>1.4 OBJECTIVE .....</b>	<b>16</b>
<b>CHAPTER 2: NILM AND CONDITION BASED MAINTENANCE .....</b>	<b>18</b>
<b>2.1 NON-INTRUSIVE LOAD MONITOR (NILM) .....</b>	<b>19</b>
<b>2.2 NILM OVERVIEW .....</b>	<b>19</b>
<b>2.3 NILM ARCHITECTURE .....</b>	<b>26</b>
<i>2.3.1 Data Acquisition Module .....</i>	<i>27</i>
<i>2.3.2 Processor .....</i>	<i>29</i>
<i>2.3.3 Event Detector .....</i>	<i>30</i>
<i>2.3.4 Diagnostics and System Management Module .....</i>	<i>30</i>
<b>2.4 NILM APPLICATIONS FOR CBM .....</b>	<b>30</b>
<i>2.4.1 Shaft Speed Harmonic Oscillation .....</i>	<i>32</i>
<b>CHAPTER 3: ALL ELECTRIC SHIP PROPULSION MODEL .....</b>	<b>47</b>
<b>3.1. NEXT GENERATION INTEGRATED POWER SYSTEMS .....</b>	<b>47</b>
<b>3.2 MEDIUM VOLTAGE DC .....</b>	<b>49</b>
<i>3.2.1 MVDC Propulsion Configuration .....</i>	<i>50</i>
<b>3.3. HARDWARE MODEL .....</b>	<b>50</b>
<i>3.3.1 Power Generation .....</i>	<i>51</i>
<i>3.3.2 Variable Frequency Drive .....</i>	<i>53</i>
<i>3.3.3 MVDC Board Description .....</i>	<i>55</i>
<b>CHAPTER 4 DOUBLY-FED MOTOR PROPULSION MODEL .....</b>	<b>61</b>
<b>4.1 THEORY .....</b>	<b>61</b>
<b>4.2 DFM PROPULSION SYSTEM OPERATION .....</b>	<b>63</b>
<b>4.2 HARDWARE MODEL .....</b>	<b>67</b>
<i>4.2.1 Doubly-Fed Motors .....</i>	<i>67</i>
<i>4.2.2 Variable Frequency Drives .....</i>	<i>69</i>
<i>4.2.3 Permanent Magnet Motor .....</i>	<i>71</i>
<i>4.2.3 Motor Cart .....</i>	<i>71</i>
<b>CHAPTER 5 CONCLUSION .....</b>	<b>79</b>
<b>5.1 SPEED HARMONIC FUTURE WORK .....</b>	<b>79</b>
<b>5.2 MVDC FUTURE WORK .....</b>	<b>79</b>
<b>5.3 DFM FUTURE WORK .....</b>	<b>79</b>
<b>WORKS CITED .....</b>	<b>80</b>
<b>APPENDIX A .....</b>	<b>82</b>
<b>GENERATOR AND MVDC BOARD OPERATING INSTRUCTIONS .....</b>	<b>83</b>

<b>APPENDIX B</b> .....	<b>98</b>
DOUBLY-FED INDUCTION MACHINE OPERATING MANUAL .....	99
<b>APPENDIX C</b> .....	<b>106</b>
MVDC BOARD MATLAB CODE .....	107
<b>APPENDIX D</b> .....	<b>117</b>
DFM WIRING SCHEMATIC .....	117
<b>APPENDIX E</b> .....	<b>118</b>
POINTS OF CONTACT .....	119



**List of Tables**

Table 1: Vibration Meter Readings for HVAC..... 37  
Table 2: Vibration Meter Readings for Lab Ventilation Fans ..... 39  
Table 3: Vibration Meter Readings for Escanaba Ventilation Fan ..... 45

**List of Figures**

Figure 1: NILM Installed in Switchboard..... 21

Figure 2: Top trace: Current drawn during the start of an incandescent lamp. Bottom trace: Stator current drawn during the start of an unloaded, fractional horsepower induction machine (7)..... 23

Figure 3: NILM Configuration for Multiple Load Monitoring (8)..... 25

Figure 4: NILM Architecture..... 27

Figure 5: Nominal quantized sin wave ..... 29

Figure 6: Simplified Electric Motor Diagram..... 32

Figure 7: HVAC Fan Lab Setup ..... 36

Figure 8: HVAC Fan Experiment FFT ..... 36

Figure 9: Lab Fan Setup..... 39

Figure 10: Shaft speed oscillation harmonic energy content for intake ventilation fan (a) and exhaust fan (b)..... 39

Figure 11: Fan Switchboard Prior to NILM Install ..... 41

Figure 12: Escanaba Ventilation Fan ..... 43

Figure 13: Escanaba FFT Plot..... 43

Figure 14: NGIPS Roadmap (13) ..... 47

Figure 15: Nominal MVDC Distribution System (15) ..... 50

Figure 16: LEES Generator Setup and Specifications..... 51

Figure 17: Coupled DC Drive Motors and Specifications..... 53

Figure 18: DC Motor Power Supplies ..... 53

Figure 19: Hitachi VFD ..... 55

Figure 20: MVDC Hardware Model..... 57

Figure 21: MVDC Board Control Circuitry..... 57

Figure 22: Bridge Rectifier Circuit and Waveforms..... 60

Figure 23: Nominal DFM Shaft Layout (18)..... 62

Figure 24: DFM Electric Circuit (16) ..... 62

Figure 25: Simplified DFM Operation Schematic (17)..... 64

Figure 26: Operating Curve for DFM (17) ..... 65

Figure 27: DFM Simulation Cart..... 67

Figure 28: DFM and Nameplate ..... 69

Figure 29: ABB ACS 355 VFDs ..... 69

Figure 30: Permanent Magnet DC Motor ..... 71

Figure 31: Optical Table Base ..... 73

Figure 32: 80/20 Box Tubing..... 73

Figure 33: T-Channel Locking Mechanism ..... 73

Figure 34: Motor Mounting Hardware ..... 75

Figure 35: Motor Base Guide Bolts ..... 77

Figure 36: Motor Base Adjustment Bolts .....	77
Figure 37: Fan/NILM Power Supply (PS1) .....	89
Figure 38: Relay Power Supply (PS2) .....	89
Figure 39: Generator Controller GUI .....	91
Figure 40: DC Motor and Field Winding Power Supplies .....	91
Figure 41: MATLAB DC ZEDs GUI .....	95

(This Page Intentionally Left Blank)

## **Chapter 1: Introduction**

### **1.1 Background**

Beginning in 1999, the Department of Defense has mandated that all military divisions develop and implement methods to reduce total ownership costs (R-TOC) of force structure and readiness. This initiative grew out of countless reviews and discussions at Program Executive Officers', Systems Command Commanders' conferences and the Defense Science Board (1). The R-TOC program was established in response to longstanding concerns about the adverse impact of defense budgetary and operational trends on force structure and readiness. Declining procurement funds due to recent defense budget cuts are resulting in a rapidly aging and potentially inefficient and unsupportable inventory. Rising operations and support (O&S) costs can consume higher portions of defense budget and leave even less available for modernization. The R-TOC program's objectives were to take actions to improve reliability and maintainability, reduce supply chain response times/footprint, and maintain or improve readiness while reducing fiscal year 2005 O&S costs by 20% or more (2).

Rear Admiral Kevin M. McCoy, the Chief Engineer of the Navy, has suggested that the Navy must focus on lowering maintenance costs for maintaining our current fleet and building an affordable future fleet (3). One measure believed to potentially save on maintenance cost is through the implementation of a condition based maintenance (CBM) program. The Navy currently uses a preventative maintenance system (PMS) for maintain the ships in the fleet. PMS is the concept of avoiding major equipment failure by providing for systematic inspection, detection, and correction of incipient failures either before they occur or before they develop into major defects through periodic inspections. While preventive maintenance is generally considered to be worthwhile, there are risks associated with conducting maintenance, i.e. equipment failure or human error involved when performing preventive maintenance. The ultimate success of the PMS program is largely based on how accurate the requirement periodicities are set; too long and the equipment fails catastrophically, too short and thousands or perhaps millions of dollars are spent needlessly on man-hours and consumables. These issues are what make CBM an attractive alternative to PMS.

Condition based maintenance is the concept of performing maintenance after one or more indicators show that equipment is going to fail or that equipment performance is deteriorating. Condition-based maintenance was introduced to try to maintain the correct equipment at the right

time. CBM is based on using real-time data to prioritize and optimize maintenance resources. Ideally condition-based maintenance will allow the maintenance personnel to do only the right things, minimizing spare parts cost, system downtime and time spent conducting maintenance.

One of the biggest challenges of integrating CBM into the modern fleet is that engineering plants in present naval vessels consist of complex networks of electrical and mechanical actuators. To facilitate new supervisory systems means that more sensors are deployed throughout the engineering plant which will in turn need to be integrated with complex algorithms. In fact, some estimates indicate that each vessel in the new DDG-1000 class will feature as many as 200,000 sensing devices (4). Although such a large sensing network may seem advantageous, it can also be both expensive and difficult to maintain and due to the level of complexity. Moreover, due to the extreme complexity of such a system, the system itself would require extensive operator training to ensure that it is operated correctly, and thus providing valuable and meaningful information. An ideal alternative would be a simple, low-cost system, with fewer sensors that could provide identical information with higher reliability. At a minimum, such an alternative could serve as a high reliability backup for an existing sensor network.

One device that can greatly simplify the supervisory monitoring and control process is the non-intrusive load monitor (NILM). The NILM is a self-contained device that can measure the current and voltage at one or more central locations in a power-distribution network. In addition to voltage and current sensing, the NILM can determine both the operating schedule and the operational status of each of the major loads in an engineering plant through transient analysis (5). NILM research is currently being conducted at the Massachusetts Institute of Technology's Laboratory for Electromagnetic and Electronic Systems (LEES). The research initiatives are exploring the application and expansion of NILM technology for the use of monitoring a myriad of electromechanical loads (i.e. making the NILM less intrusive while maintaining all existing capability). Furthermore, the NILM can also use its electrical data to assess the status of certain mechanical elements such as air filters in ventilation systems. The NILM's potential to disaggregate individual loads from bus current and voltage may provide future electrical protection systems with valuable information to protect critical loads.

## **1.2 U.S. Coast Guard Initiatives**

In addition to the United States Navy making instrumenting programs to make maintenance more cost effective, the United States Coast Guard (USCG) is investigating efforts in making their maintenance practices more efficient. The USCG currently uses vibration analysis to assess a particular electric machine's condition such as bearing faults, misalignment, imbalance, electrical faults and several other potentially damaging faults (6). The present method of vibration monitoring requires mounting a sensor to the outer hub of the motor and taking readings from a handheld vibration meter. One concern with this method involves the position of the transducer that is placed on the outer hub. A preliminary study by Thomson et al. showed that stator frame vibration changes as a function of the transducer position around the periphery of the frame (7). There is no procedure in place to ensure that the transducer will be placed at the same location each occasion the measurement is conducted. Without such consistency the maintenance check thus the accuracy of these readings over time will not be as reliable as they should be. Also, this method requires manned inspection which is more costly than and automated systems. Additionally, these vibration checks are conducted periodically which may not be frequent enough to catch any serious, potentially fatal, damage in a motor. Electrical-based vibration monitoring could overcome some of these shortcomings. By monitoring the current drawn by the motor, the data recorded are less prone to operator error. Electrical-based monitoring can be automated so that a computer can track the vibration of the motor on a near continuous basis. Electrical-based vibration monitoring might eliminate the need for outside experts as the analysis can be done continuously by a computer.

## **1.3 U.S. Navy Initiatives**

In addition to evaluating cost saving by the implementation of CBM, the USN has undertaken steps to reduce life-cycle costs of their vessels. One method in which these objectives are being achieved is through the implementation of an integrated power system (IPS). IPS is a concept that is currently being explored by the US Navy that will provide the ability for electric propulsion and ship service electrical loads to be driven from a common power source. This ability to draw both propulsion and hotel load power from one common source allows provides the commanding officer with energy for other uses (i.e. high energy weaponry) when high-speed propulsion is not an operational requirement. It is also believed that this arrangement could assist in obtaining better fuel economy due to the ability run the gas turbine generators at their

most efficient speeds continuously and independent of the ships current task. Furthermore, this “open” architecture makes the installation of future upgrades more flexible; with IPS the operator can sacrifice a ship’s maximum transiting speed to allow for the installation of a new high power consumption radar system.

While the advent of IPS provides the operators with a very unique capability, the main question becomes how to most effectively integrate the propulsion and electrical systems to provide not only a system that is efficient, but one that is also robust and will withstand the failure in the event of a casualty. Current proposals suggests that converting all power generations sources to medium voltage DC (MVDC) is the best solution, however, this solution requires a significant amount of power electronics for the conversion and distribution of DC power. An alternative is to providing propulsion from an AC electric bus through the use of a doubly fed machine. This method has the potential to significantly reduce the number of power electronics cabinets and provide a more robust architecture for which to base the IPS system.

#### **1.4 Objective**

This thesis consists of five chapters including the introduction and conclusions. Chapter 2 takes an in-depth look at the non-intrusive load monitor and how it can be used as a tool for CBM. This chapter is meant to give insight on how the NILM is constructed, its functionality, and how the information collected by the NILM can be used in a shipboard environment. Experiments conducted in in LEES as well as aboard the USCGC ESCANABA (WMEC-907) will be used for validating the proposed methodology. Chapter 3 delves into the derivation of prolusion power from a MVDC integrated power system. This chapter discusses the pros and cons of the MVDC configuration as well as the construction of the hardware model that cannot only be used to simulate propulsion from an MVDC bus, but also encompasses the ability to be used as a test platform for future experimentation which may require vast amounts of DC power. Chapter 4 will explore the derivation of propulsion power from an AC power system through the use of a doubly-fed induction machine. This chapter will summarize benefits and drawbacks to such a configuration and the construction of the hardware model constructed from concept exploration. The final chapter will summarize the findings and detail areas for further research.

The goals of this thesis were to:



- proposes a method for electrical-based condition monitoring using shaft speed oscillation harmonics to assess the health of an electrical load
- Construct a hardware model of an IPS propulsion system that can be used to test various IPS propulsion concepts

(This Page Intentionally Left Blank)

## **Chapter 2: NILM and Condition Based Maintenance**

### **2.1 Non-Intrusive Load Monitor (NILM)**

The non-intrusive load monitor (NILM) is a device used to measure raw current and voltage from a single point in an electrical distribution system. Non-intrusive load monitoring research has been conducted at Massachusetts Institute of Technology's Laboratory for Electromagnetic and Electronic Systems (LEES) over the past two decades. The main focus of this research has been to understand how the dynamics of various shipboard systems can be monitored using NILM and their operating modes and failure modes detected. The performance of important electro-mechanical loads on mission-critical systems contained inside power plants as well as aboard warships is often tracked by dedicated monitoring equipment. These systems can at times be extremely large, taking up valuable real-estate and require significant training for the operators, thus mitigating the cost benefit from owning such a system. The advantage of non-intrusive load monitoring over conventional load monitoring is the ease of installation at the site. This is due to the NILM needing voltage and current from a single aggregate profile to determine the operating characteristics of several loads. Additionally, the NILM offers simplification of data collection given that it automatically determines the electrical nature of the load due to onboard processing algorithms. Furthermore, the NILM enhances evaluation of data since the NILM collects and can potentially analyze data at one centralized location. NILM uses can be divided into two broad categories: transient and steady-state approaches. The transient approach finds loads by examining the full detail of their transient behavior. This type of analysis is useful if loads are continuously being started and stopped, such as a hydraulically operated door. Dynamic changes in the power and harmonic consumption of a load, such as turn-on or turn-off transients, can serve as a fingerprint for identifying load operation. The steady-state approach focuses more on observing operations over long period of time to detect anomalies. The steady state analysis can provide the end user with priceless data that can be used to determine the exact mode of failure for a particular piece for equipment. Currently the NILM is being commercially used in residential, industrial and automotive environments (8).

### **2.2 NILM Overview**

The NILM is constructed from lower cost Commercial-off-the-Shelf (COTS) equipment with custom sensor boards and software. It consists of two major components, an electrical enclosure that processes sensor inputs and a computer that analyzes the output. On a 3-phase system, the

(This Page Intentionally Left Blank)

typical inputs to the electrical enclosure are one current transducer, used to measure the aggregate current, and two voltages taps that are used to determine the voltage between two phases of a multi-phased electrical distribution system.

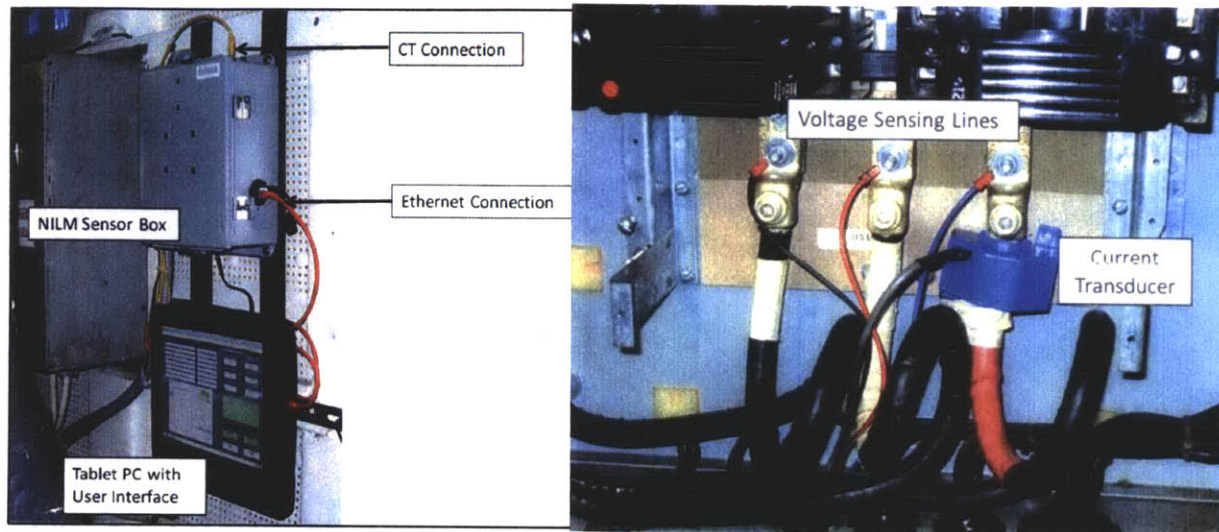


Figure 1: NILM Installed in Switchboard

The NILM measures the aggregate current flowing to a bank of electrical loads. It then disaggregates the operating schedule of individual loads through the use of Fourier Transforms and current spectrum analysis. The electronics in the electrical enclosure collects these measurements and sends them to the computer where the real and reactive powers are calculated along with their associated harmonics. These measurements can be used to perform diagnostics on the electrical system and/or determine the operating schedule of major electrical loads. As shown in Figure 2, for example, the physical differences between an incandescent lamp and an induction machine result in vastly different transient patterns.

(This Page Intentionally Left Blank)

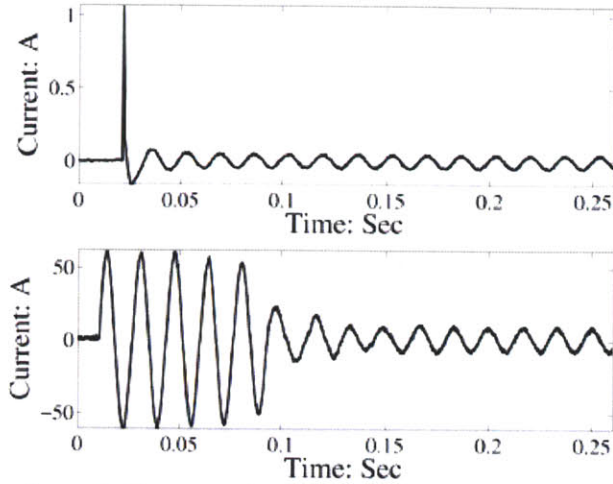


Figure 2: Top trace: Current drawn during the start of an incandescent lamp. Bottom trace: Stator current drawn during the start of an unloaded, fractional horsepower induction machine (7)

Additionally, the NILM can use these measurements to diagnose impending failures in the mechanical systems that are actuated by the electronics. When applied to a given electro-mechanical system, the power measurements provide vital system information that can be used to determine the overall "health" of not only the electrical components (i.e. motors), but also the mechanical components (i.e. pumps, filters, valves, etc.) of a given system. The NILM can also monitor the operation of the electrical distribution system itself, identifying situations where two or more otherwise healthy loads interfere with each other's operation through voltage waveform distortion or power quality problems.

Figure 3 shows a nominal NILM layout where multiple loads are monitored via a single NILM. While the ideas of having a single NILM perform diagnostic monitoring of an entire ship or power plant are advantageous, the algorithm needed to effectively perform such tasks as event detection and system diagnostics is not trivial. As the NILM moves farther upstream to monitor multiple loads from a single point, it becomes less intrusive. Placing the NILM too far upstream would result in an onslaught of data recording that would not provide the user with any useful data. On the other hand, placing a single NILM on every load would provide great resolution on every load's operating condition, but would not be cost or space efficient. Due to these aspects there are limitations to how far upstream or downstream the NILM can be installed and conduct both transient and steady state analysis effectively. The ultimate goal of NILM is to provide the user real time, useful information that

(This Page Intentionally Left Blank)



can extend the life and lower the cost of maintaining equipment, without the use of a complex physical sensor network.

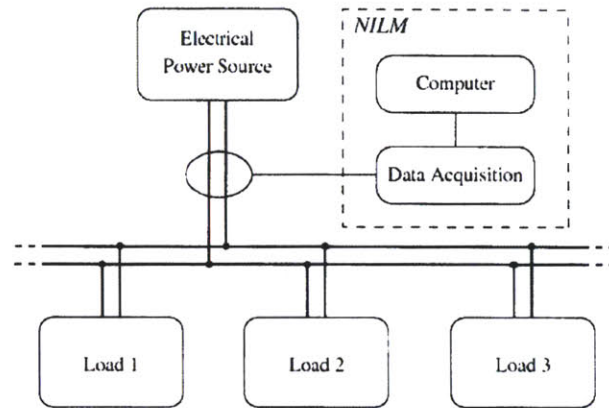


Figure 3: NILM Configuration for Multiple Load Monitoring (8)

In addition to the NLM’s installation location, there are several other factors that influence the NILM's ability to perform aggregate diagnostic monitoring: First are the limitations of the digital to analog converters used in the NILM. During operation the NILM samples a continuous signal which must be converted into finite digital data output which results in quantization. Quantization errors can affect how accurately the incoming signal is transmitted to the processor. Secondly are the limitations of the power monitoring components used to manufacture the NILM. For a given NILM hardware configuration, the power range it observes is bounded by the sensor and analog to digital card selection. Locating the NILM closer to the power source results in a different hardware selection to account for the larger power range being observed, therefore, decreasing the NILMs sensitivity to accurately detect smaller transients. Third is the NILMs susceptibility to electrical noise from the loads that are being monitored. Locating the NILM greater distances from the load significantly increases the channels for noise interjection. Lastly is the NILM’s ability to disaggregate similar load powered from a common supply, The NILM must encompass the ability to disaggregate similar loads in order to offer an effective means of observing potentially catastrophic events. Given that two identical motors are powered from the same source, the aggregate voltage and current levels alone may not be enough to resolve the two loads. From a designer's perspective, these are necessary tradeoffs that impact the NILM's performance in real world applications.

(This Page Intentionally Left Blank)

### 2.3 NILM Architecture

Figure 4 shows the block diagram of a standard NILM and an internal view of the NILM sensor box as it is configured today. A typical NILM configuration consists of an enclosed sensor box which houses the data acquisition module, the preprocessor, the event detector, a data storage unit and the diagnostic and systems management module, external power connections (current transducers and voltage sensing lines), and a personal laptop computer for data processing and archiving. Power to the internal electronics of the NILM is typically drawn from the switchboard in which it is installed.

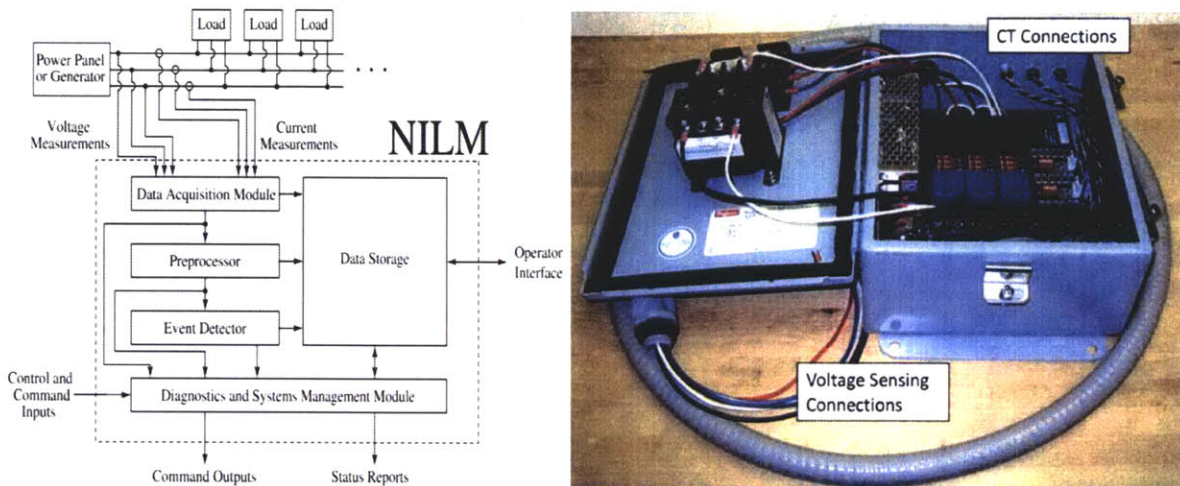


Figure 4: NILM Architecture

#### 2.3.1 Data Acquisition Module

There are many different data acquisition modules available on the market. They are used in different applications and have various numbers of inputs or outputs. The data acquisition module provides the I/O capabilities for current and voltage seen by a particular load or group of loads within a system. A majority of the information that is used for NILM applications is derived from the current signal. Acquired data is converted into digital form through an analog-to-digital converter. The data acquisition module uses a phase-locked, short-time Fourier transform of current waveforms collected at sample rates of 8,000 Hz or higher to compute spectral envelopes that summarize time-varying harmonic content. The high sample rate ensures that error introduced from the analog to digital conversion is maintained to a minimum.

(This Page Intentionally Left Blank)

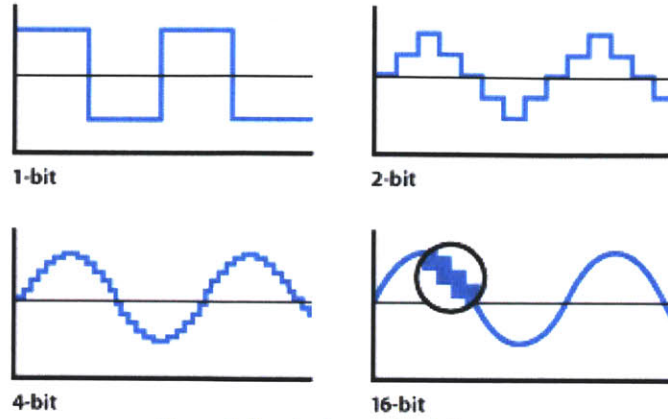


Figure 5: Nominal quantized sin wave

The number of quantization levels can be derived based on the number of significant binary bits available for a particular analog-to-digital conversion card. As can be seen in the figure above, the greater the number of bits available the more precise the quantized signal becomes. The quantized signal from the converter is passed to a processor for preprocessing.

### 2.3.2 Processor

The preprocessor extracts useful information from the raw data signal for detection, classification, and diagnostic functions. Similar to radio transmissions using amplitude modulation, the target information is carried on a 60Hz (for typical shipboard distribution systems) waveform with varying amplitude. The carrier waveform is removed, revealing the power spectrum and its vital information. The resulting envelope is used to identify loads and perform diagnostics. These spectral envelopes are defined as:

$$x(t - T + s) = \sum_k a_k(t) \cos(k \frac{2\pi}{T} (t - T + s)) + \sum_k b_k(t) \sin(k \frac{2\pi}{T} (t - T + s)) \quad (1)$$

The coefficients  $a_k(t)$  and  $b_k(t)$  are the spectral envelopes of  $x$  for the harmonic  $k$ . The coefficients  $a_k(t)$  and  $b_k(t)$  can be found from the following formulas (10):

$$a_k(t) = \frac{2}{T} \int_0^T x(t - T + s) \cos(k \frac{2\pi}{T} (t - T + s)) ds \quad (2)$$

$$b_k(t) = \frac{2}{T} \int_0^T x(t - T + s) \sin(k \frac{2\pi}{T} (t - T + s)) ds \quad (3)$$

The spectral envelopes computed by the preprocessor are passed to an event detector that identifies the operation of each of the major loads on the monitored electrical service. In the current revision of the NILM, load identification and analysis is conducted using both transient and steady-state information (5). Field studies have demonstrated that transient details are particularly powerful because the transient electrical behavior of a particular load is strongly influenced by the physical task it performs (8).

### 2.3.3 Event Detector

The spectral envelopes computed by the preprocessor are passed to an event detector that identifies the operation of each of the major loads on the monitored electrical service. The event detector has no prior knowledge of the operating schedule for the loads; however it contains the capability to detect, classify, and diagnose load transients. The transient behavior of many important load classes is sufficiently distinctive to serve as a reliable indicator of load type.

### 2.3.4 Diagnostics and System Management Module

The final block is the NILM is the diagnostics and systems management module. This software unit assesses load status using any required combination of current data, voltage data, spectral envelopes, and load operating schedules (9). Diagnostics require accurate classification of transients within a monitored system. Once properly identified, algorithms can be used to look for "unusual" behavior.

## 2.4 NILM Applications for CBM

In conjunction with total ownership cost reduction due to manufacturing ships with flexible IPS architectures, the Navy is evaluating the ability to springboard these efforts to reduce manning aboard its vessels. The reduction in shipboard crew manning inherently results in an increase in automation and a fundamental shift in current Navy maintenance practices. Previously, the Navy used a Preventative Maintenance System (PMS) where maintenance on equipment was conducted at scheduled regular intervals. In many cases the scheduled maintenance includes disassembly and inspection whether or not the equipment exhibited signs of malfunction. This is

not only manpower intensive but also costly. For example, upon assembly new expendable parts (i.e. seals and gaskets) would be installed and the old ones, often still in good working order, discarded. This maintenance practice, while proven effective, is by far not the most efficient. One of the initiatives for increasing maintenance efficiency is through the use of Condition Based Maintenance (CBM). This philosophy abandons the old, scheduled PMS whereby maintenance is conducted independent of the equipment's condition and maintenance is conducted when equipment exhibits symptoms of imminent failure (i.e. reduced output, vibrations, etc.). This type of philosophy results in a reduction in maintenance related man-hours. In addition, the Navy is shifting most many of its maintenance practices away from the organizational level and placing the burden on the shore maintenance personnel for the new modern warship. Less man-hours required for maintenance translates to less manpower requirements overall and ultimately a reduction in vessel manning, as the smaller crew can now be gainfully employed conducting other war fighting tasks.

In addition to the Navy's maintenance cost reduction measures, the United States Coast Guard is currently investigating methods to reduce costs of its vibration monitoring program. The United States Coast Guard uses vibration analysis to assess a particular electric machine's condition such as bearing faults, misalignment, imbalance, electrical faults and several other potentially damaging faults in lieu of a dedicated PMS regiment (6). While this approach is more efficient than conducting maintenance on a purely periodic basis, there are a number of shortfalls to this system. First, it requires someone familiar with the vibration monitoring process and appropriate training to travel to the ship, configure the target system for analysis, run the test (usually more than once), record the data, and return to enter the data in the appropriate data base. Even after the data has been recorded, this technique still requires the user to have some degree of expertise in order to distinguish a normal operating condition from a potential failure mode. Additionally, there is no guarantee that the transducer will be placed at the same exact location each time there is a maintenance check. Without this consistency, trend analysis cannot be conducted, thus essentially making the data useless for long-term trend analysis. It is believed that the NILM can be used to alleviate these concerns through the monitoring of the electrical supply to the load. By monitoring the current drawn by the motor, the data recorded are less prone to operator error. Additionally, with electrical based monitoring the process can be automated. This automation

will ensure that the data for long term trend analysis is recorded and available for examination in the event of a failure. Finally, electrical-based vibration monitoring might eliminate the need and cost associated with outside experts as the analysis can be done “in-house” by a computer.

### 2.4.1 Shaft Speed Harmonic Oscillation

Vibration analysis has been used for countless years to assess a particular machine’s condition including bearing faults, misalignment, imbalance, electrical faults and several other potentially damaging faults. It has been shown that current and voltage waveform of an operating piece of machinery machine can be used for electrical based vibration analyses through the use of the machines shaft speed oscillation harmonic. The shaft speed oscillation harmonic provides a reliable way to monitor stator frame vibration.

#### 2.4.1.1 What is Shaft Speed Harmonic Oscillation?

Shaft speed oscillation is a dynamic eccentricity that varies with rotor position. Rotor asymmetry resulting from a faulty bearing, rotor ellipticity, misalignment of the shaft with the cage results in vibrations and oscillations in the current waveform. The figure below is a simplified representation of an induction motor figure A is a motor with new bearings and figure B shows a motor with bearings near the end of their useful life.

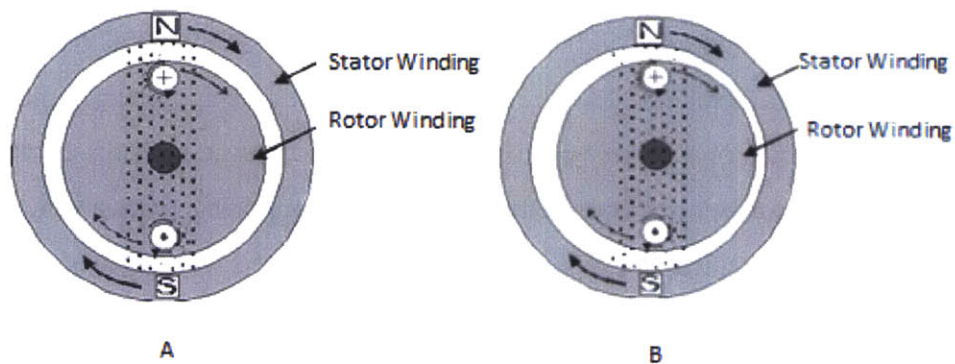


Figure 6: Simplified Electric Motor Diagram

As can be seen in figure B, as the motor turns, the rotor slots alter the effective length of the air gap sinusoidally thereby affecting the permeance of the machine. This sinusoidal behavior is seen in the flux, which is the product of the magnetomotive force (MMF) and the permeance across the air gap.

$$\phi = \mathcal{F}\Lambda \tag{4}$$



Static and dynamic eccentricity harmonics also appear in the stator current as the rotor turns irregularly in relation to the stator. These fluctuations result in sinusoidal current and voltage waveforms that can be analyzed by the NILM and thus used to determine the condition of a rotating piece of machinery.

Previous research has been done to study the effects of mechanical faults on the stator current spectrum. These faults, including broken rotors bars, damaged bearings, rotor eccentricity, rotor asymmetry, bearings failures, and shaft speed oscillations, produce distinct harmonics in the current spectrum. It has been discovered that the current spectrum contains potential fault information for such events (10). Frequency components, which are derived from the physical construction of the machine, have been determined for each specified fault. It is important to note that, just as in vibration analysis, as the fault progresses, its characteristic spectral components continue to increase over time. For example, mechanical vibrations in induction machines can be associated with variations in the physical air gap of the motor (11). These effects cause a slow variation in the torque produced by the machine, and thus induce a corresponding variation in the amplitude of its current. The detection of such modulation can be extremely useful from a diagnostic perspective.

#### **2.4.1.2 Shaft Speed Harmonic application to CBM**

It is believed that the NILM can be used to monitor the vibration through the use of current sensing. The vision of the NILM is that a minimal number of sensors will eventually be used to monitor multiple loads, but the algorithm to perform this task automatically may prove to be extremely complex. This is because the monitored spectral components can result from a number of sources, including those related to normal operating conditions. This requirement is even more acute when analyzing the current spectrum of an induction motor since a multitude of harmonics exists due to both the design and construction of the motor and the variation in the driven load. Many of these harmonics can be caused by non-circularities in the rotor, voids in the casting, slot design, etc.

Current versions of the NILM identify loads simply by looking at transient patterns and steady-state power changes. This may not be enough when looking at multiple systems. One option that will be investigated is the use of system spectral information. Analogous to the mechanical

vibration monitoring, the electrical spectral information presents a greater potential for multi-system remote monitoring and overall cost savings. By monitoring the current drawn by the motor, the data recorded are less prone to operator error. Electrical-based monitoring can be automated so that a computer can track the vibration of the motor more regularly. Finally, electrical-based vibration monitoring might eliminate the need for outside experts as the analysis can be done “in-house” by a computer.

#### 2.4.1.2.1 Shaft Speed Model

To begin developing a model to predict the location of shaft speed oscillation harmonics in the motor current spectrum, a simplified steady-state equivalent circuit is used to model an induction motor. The following derivation is adapted from (12).

The shaft speed of the motor is assumed to be comprised of an average speed and a sinusoidally-varying component given by Eq. (1).

$$n(t) = N_r + \sum_k N_k \sin(2\pi k f_c t) \quad (5)$$

Where  $N_r$  is the motor’s rotational speed in rotations per minute,  $N_k$  is the Fourier component of the speed fluctuation, and  $f_c$  is fundamental frequency of the speed fluctuation. The rotational speed  $N_r$  can be calculated as

$$N_r = \frac{60}{p} \cdot \frac{\omega_r}{2\pi} \quad (6)$$

Where  $\omega_r$  is the rotational frequency in radians per second and  $p$  is the number of pole pairs. The relative phases between the sinusoids are ignored in this derivation. The line voltage is modeled as a pure sine wave at the line frequency, given by Eq. (3).

$$v(t) = V \sin(2\pi ft) \quad (7)$$

Where  $V$  is the voltage amplitude and  $f$  is the voltage line frequency. The underlying assumption for  $f_c$  is that the shaft speed oscillation is periodic with the position of the shaft. Thus, this phenomenon produces stator current harmonics with frequencies predicted by

$$i_s(t) = \frac{v(t)}{r(s)} \quad (8)$$

Where  $r(s)$  is the slip-dependent rotor resistance and is expressed as  $\frac{R}{s}$  for some nominal resistance  $R$  and slip  $s$ . The slip  $s$  of the motor is defined as

$$s = \frac{N_{\text{sync}} - n(t)}{N_{\text{sync}}} \quad (9)$$

Where  $N_{\text{sync}}$  is the synchronous speed of the motor. The synchronous speed  $N_{\text{sync}}$  can be calculated as

$$N_{\text{sync}} = \frac{60}{p} \cdot \frac{\omega}{2\pi} \quad (10)$$

Where  $\omega$  is the stator electrical frequency in radians per second. Combining (1) - (6) and using the product of sines trigonometric identity, the line current  $i_s(t)$  has a line frequency component which is present from the non-varying speed component of the rotor. The other terms are symmetric sidebands which arise from the shaft speed variation. These shaft speed oscillation harmonics are expressed by

$$f_{\text{SSO}} = f \left[ k \left( \frac{1-s}{p} \right) \pm 1 \right] \quad (11)$$

Where  $s$  is per unit slip,  $k = 0, 1, 2, \dots$  and  $p$  is the number of pole pairs. It is believed that the shaft speed harmonics can be used as a method to evaluate the condition rotating machinery.

#### 2.4.1.2.2 Lab Experiment Setup and Results

To verify the expression in Eq. (9), an experiment using a heating, ventilation and air conditioning (HVAC) unit was conducted. A 3 phase, 3 pole-pair ( $p = 3$ ) induction machine was

outfitted with an evaporator fan in a heating, ventilation and air conditioning (HVAC) unit. Additional weight was placed on the fan to create an imbalance to induce more vibration. A current transducer was placed around one of the phases and thirty seconds of data were recorded for each incremental weight added.

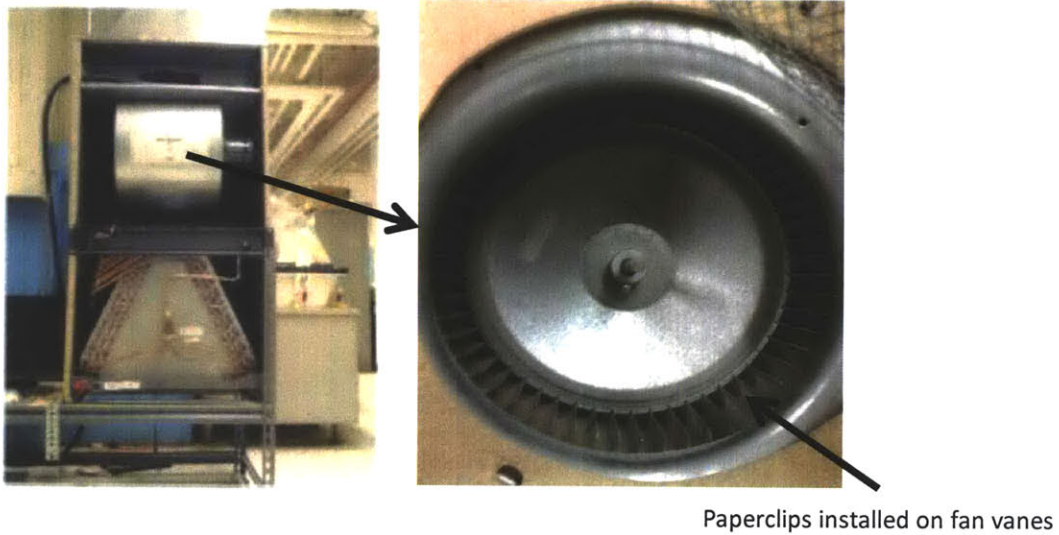


Figure 7: HVAC Fan Lab Setup

A fast Fourier transform (FFT) was taken on the data to compute the spectral content. For this motor, with  $p = 3$  and for a low-slip assumption ( $s < .05$ ) and a  $f = 60$  Hz supply line frequency, the principal shaft speed oscillation ( $k = 1$ ) is between 79 Hz and 80 Hz. Figure 8 displays the frequency content of the motor for different amounts of weights or clips.

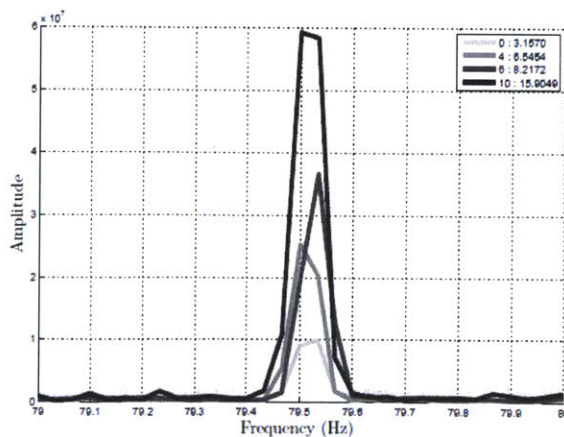


Figure 8: HVAC Fan Experiment FFT

Number Of Clips	Vibration Reading (g)	Normalized Energy
0	.03	3.15
4	.09	6.54
6	.10	8.21
10	.19	15.90

Table 1 lists the normalized energy content in the frequency window shown in Figure 8. The energy is calculated by integrating the total amount of spectral content in the inspection window. The second column displays the reading from an Extech 407860 Heavy Duty Vibration Meter in units of g. The results show that the energy from the shaft speed oscillation harmonic correlate well with radial vibration.

Number Of Clips	Vibration Reading (g)	Normalized Energy
0	.03	3.15
4	.09	6.54
6	.10	8.21
10	.19	15.90

Table 1: Vibration Meter Readings for HVAC

A second experiment was conducted on a pair of single phase ventilation fans loaned by the Industrial Electric Shop (IES) on the 1st District Coast Guard base in Boston, Massachusetts. These machines were previously used for intake and exhaust ventilation in the main engine room aboard one of the Coast Guard's 49 ft buoy boats. For these motors, with  $p = 1$  and for low-slip assumption ( $s < .05$ ) and an  $f = 60$  Hz supply frequency, the principal ( $k = 1$ ) shaft speed oscillation harmonics are between 117 Hz and 120 Hz. To avoid the 120 Hz supply harmonic, the window of inspection included the frequencies between 117 and 119 Hz. Each motor was turned on independently and recorded for 30 seconds. Figure 3 graphs the frequency content of the intake (3(a)) and exhaust fans (3(b)) for different amounts of weight. Data were taken under "normal" conditions, with a small weight ("little screw") and a larger weight ("big screw") attached to the hub of the fan.

(This Page Intentionally Left Blank)

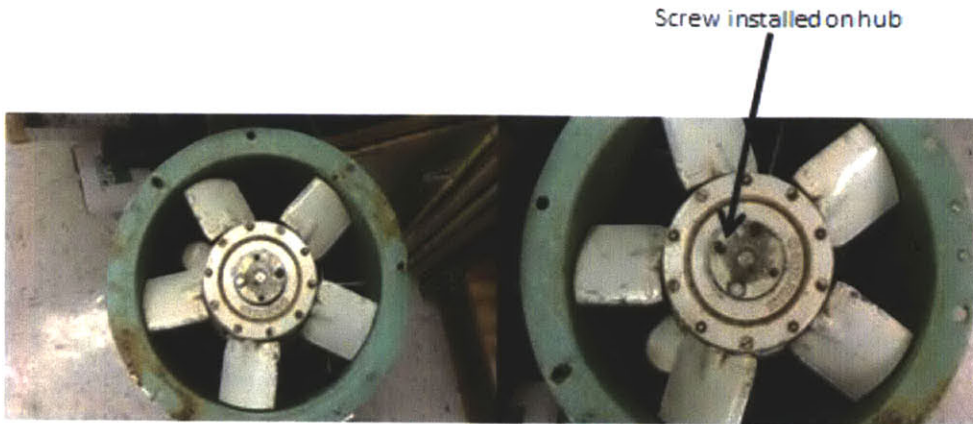


Figure 9: Lab Fan Setup

Figure 3 graphs the frequency content of the intake (3(a)) and exhaust fans (3(b)) for different amounts of weight. Data were taken under “normal” conditions, with a small weight (“little screw”) and a larger weight (“big screw”) attached to the hub of the fan.

Eccentric Condition	Intake Fan Data		Exhaust Fan Data	
	Vibration Reading (g)	Normalized Energy	Vibration Reading (g)	Normalized Energy
Normal	.37	2.81	.78	4.09
Little Screw	.47	3.46	1.09	4.38
Big Screw	.59	3.91	1.15	4.69

Table 2: Vibration Meter Readings for Lab Ventilation Fans

lists the normalized energy content in the frequency window for the ventilation fans. The vibration readings were recorded from an Extech 407860 Heavy Duty Vibration Meter in units of g. The results show that the energy from the shaft speed oscillation harmonic correlates well with radial vibration.

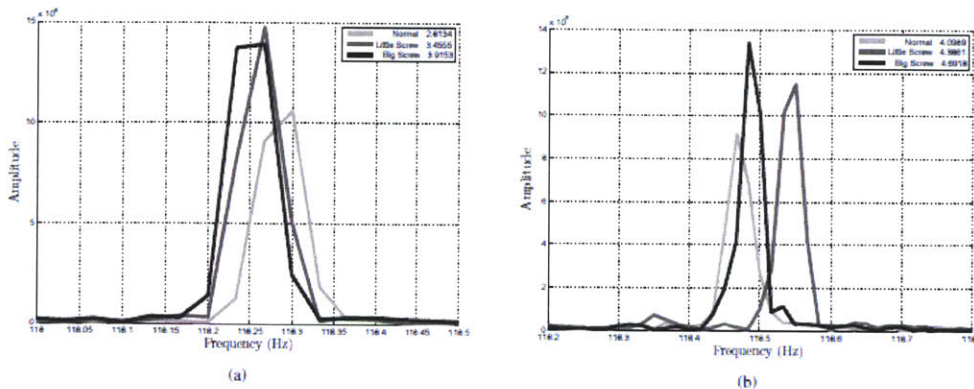


Figure 10: Shaft speed oscillation harmonic energy content for intake ventilation fan (a) and exhaust fan (b)

(This Page Intentionally Left Blank)



### 2.2.3 Escanaba Experiment Setup and Result

After verifying the theory of using speed harmonic oscillation to monitor for radial vibrations in the controlled environment of the LEES lab, it was decided to further validate the theory by testing it in the field. For the field experiments we conducted aboard the US Coast Guard Cutter Escanaba (WMEC-907). For consistency with the lab experiments, a fan was selected with similar specifications to the lab ventilations fans was used. For data recording the NILM was installed in the fan controller.

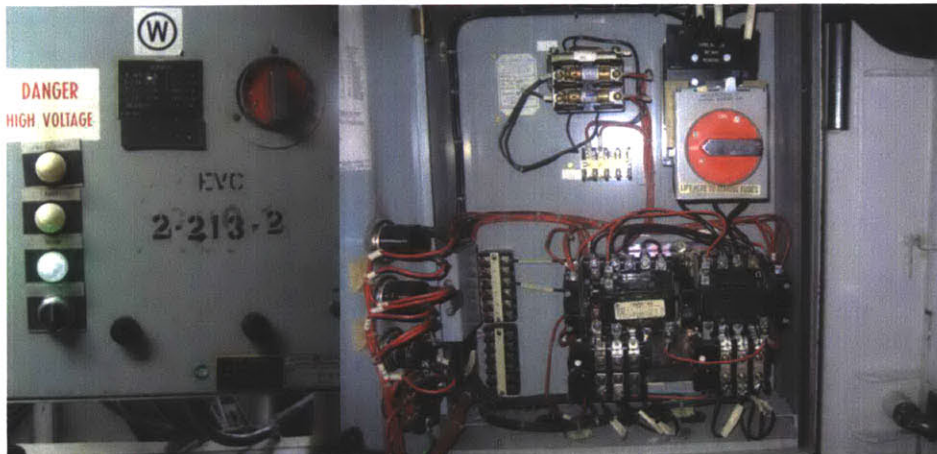


Figure 11: Fan Switchboard Prior to NILM Install

Similar to the experiments conducted in the lab, the experiments conducted aboard the Escanaba involved introducing a small eccentricity into the ventilation fan and recording the current waveforms for several different eccentricities. While the installation of different sized screw in the hub was desired for consistency between the two experiments, the hub design of the fan was slightly different preventing the installation of the screw. Instead several coils of wire were wound around a single fan blade to introduce eccentricity in the Escanaba fan motors.

(This Page Intentionally Left Blank)

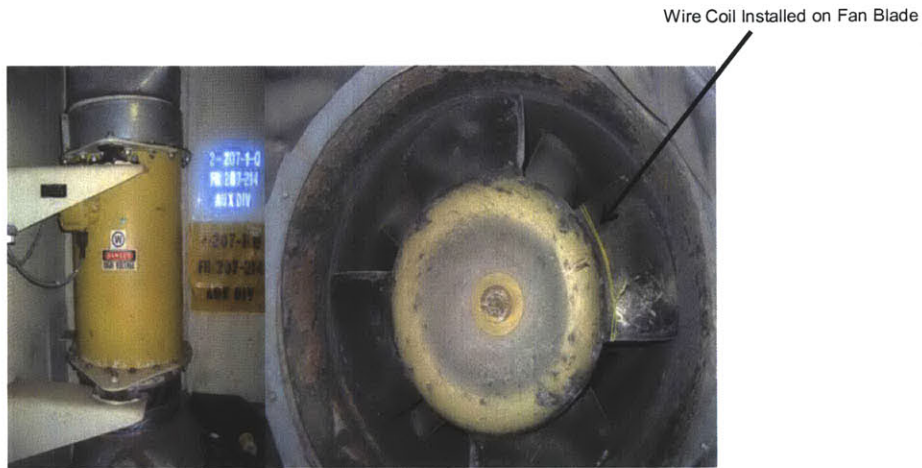


Figure 12: Escanaba Ventilation Fan

Following each data run additional coils were placed on the fan to create an imbalance to induce more vibration. A current transducer was placed around one of the phases and thirty seconds of data were recorded for each incremental weight added. A total of five data runs were conducted, no eccentricity, 2 coils, 4 coils, 6 coils and 8 coils added.

Shown in Figure 13 is the data obtained for the five data runs collected. As can be seen from the data contained in Figure 13 and Table 3, the data does not correlate well with the vibrations readings obtained from the handheld meter. The energy found from the FFT of the speed harmonic oscillation method appears to be indiscriminate.

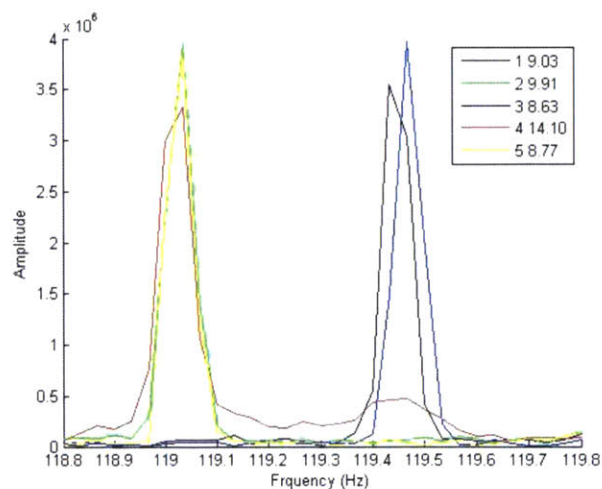


Figure 13: Escanaba FFT Plot

(This Page Intentionally Left Blank)

The vibration data found in Table 3 shows an increasing trend with the increase amount of eccentricity introduced from the coils of wire.

<b>Coils of Wire</b>	<b>Vibration Reading (g)</b>	<b>Normalized Energy</b>
<b>0</b>	<b>.20</b>	<b>9.03</b>
<b>2</b>	<b>.26</b>	<b>9.91</b>
<b>4</b>	<b>.38</b>	<b>8.63</b>
<b>6</b>	<b>.55</b>	<b>14.10</b>
<b>8</b>	<b>.68</b>	<b>8.77</b>

**Table 3: Vibration Meter Readings for Escanaba Ventilation Fan**

There are several possibilities that could explain why the field data does not correlate with the vibration meter readings as well as the lab data. One theory is the fact that there are several cycling loads on aboard the Escanaba. These loads can interject harmonics that can constructively or destructively interfere with the shaft speed harmonic of the target load, thus rendering the data useless for condition analysis. When two or more motors are loading the utility line, the voltage amplitude drops and this slows down the motors. This slip difference also changes the total energy content from the shaft speed oscillation harmonic. One possible explanation is when the slip changes, the motor is operating at a new point on its torque-speed curve. Each point on the curve may react differently to eccentric weight depending on the torque turning the shaft.

A second theory is that the wire used to introduce the eccentricity is so lightweight that its mass is not significant enough to introduce a speed harmonic oscillation. Ducted fans all contain three parts: a fan, a motor, and the duct pipe section. The fan is rigidly attached to the shaft of the motor forming the fan/rotor assembly. The fan/rotor assembly is secured axially and radially to the motor by a pair of deep groove ball bearings. Ball bearings, primarily through the flexibility of their constituent materials, possess a radial stiffness that can be modeled as a linear spring and damper in parallel. The motor body in a ducted fan is rigidly attached to the duct pipe section, while the duct pipe section is often attached to low stiffness but highly dampening vibration isolation mounts which secure the unit to the surrounding structure.

The experiments conducted have demonstrated that the shaft speed oscillation harmonics can serve as an electrical-based vibration reading for monitoring the health of motors. Results from

experiments in a laboratory environment were consistent with this claim. Based on the field data it was determined that there are some limitations to these methods. It was shown that in a multi-load environment the slips of each load to decrease due to voltage droop. A robust algorithm will need to take this phenomenon into consideration.

## Chapter 3: All Electric Ship Propulsion Model

### 3.1. Next Generation Integrated Power Systems

In response to the DoD directive to develop methods to cut defense budget spending, the Navy is directing efforts towards the development of ships that make more efficient use of on-board power and to cut fuel use. To assist in these efforts, new technologies are being explored that will allow the propulsion power and hotel loads to be driven from one common power source using an Integrated Power Systems (IPS). An added benefit to such a system is the ease of which future high-power weapons such as the electromagnetic gun, high power microwave and high energy lasers can be integrated. To provide direction for future IPS development, The Navy initiated the Next Generation Integrated Power Systems (NGIPS) effort. The figure below depicts the roadmap for the advancement of IPS.

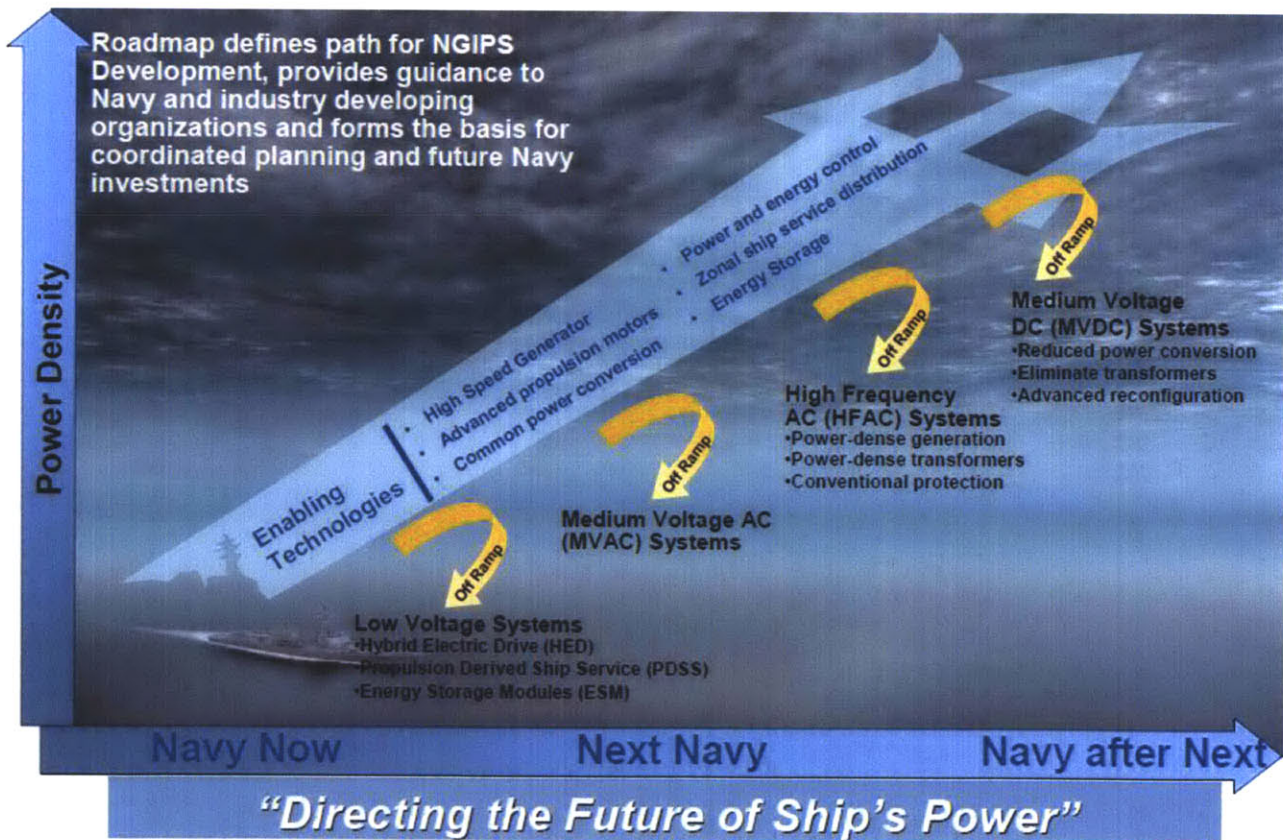


Figure 14: NGIPS Roadmap (13)

(This Page Intentionally Left Blank)



### **3.2 Medium Voltage DC**

Medium Voltage DC (MVDC) Power Generation is the long term goal for providing affordable power dense systems aboard Navy combatants. The MVDC distributed power will likely employ balanced voltages in the range of  $\pm 3,000$  VDC to  $\pm 10,000$  VDC (13). There are several reasons why an MVDC distribution system is attractive. First, the use of a DC distribution system decouples the speed of the prime mover from the frequency of the bus. This allows for generator to be optimized to a particular prime mover eliminating the need to incorporate reduction gears to maintain a certain bus frequency. Secondly, DC power greatly reduces the concern for electromagnetic interference (EMI). This EMI reduction not only minimizes interference and cross talk between components, it also reduces the ships susceptibility to be detected through passive measures. Along with a reduction in the EMI signature, there can also be an acoustic benefit gained from a DC distribution system. Since there is not a common frequency of vibrating equipment, the acoustic signature has a broader signature with fewer tonals that can be observed in the acoustic signature of the ship. A DC distribution system also provides the operator with a system that is much simpler to operate. The paralleling of generators would only require voltage matching.

While the use of MVDC aboard warships seems advantageous, its benefit does not come free from any disadvantages. While fault detection and isolation in an AC distribution system can be accomplished using conventional AC circuit breakers, their use in a DC distribution system is not desirable. This is due to the difficulty in extinguishing DC arcs in the absence of a voltage or current zero crossing. However, this problem can be possibly remedied through the use of advanced power electronic devices that are capable of quickly identifying and isolating faults before large fault currents are generated, but these systems require significant R&D to perform with the desired reliability. Furthermore, there is no industrial base for building the MVDC components. The DC Switchgear as well as the power electronic fault detection and control systems needed to make shipboard MVDC systems viable have an insignificant commercial market. Consequently, the Navy will have to rely on a small industrial base of vendors with MVDC experience and will have to actively address risks associated with the loss of a key vendor through such methods as large number of contingency spares and establishing a large in-house engineering capability (14). In addition to the establishment of an industrial base, changes would also have to be made to shore facilities. When the ship is in port the pier will need to

encompass the ability to provide the ship with MVDC. An alternative to modifying the shore facilities would be to house the reciter aboard the ship. However this solution is unattractive due to the considerable amount of internal real estate that will be compromised to accommodate machinery to support the brief in-port periods of a typical combatant.

### 3.2.1 MVDC Propulsion Configuration

The schematic below illustrates the arrangement of a nominal MVDC distribution system. To create the DC power system, two AC rotating machines are utilized. The electrical output of each of these machines is rectified and used to energize one of the two DC busses. The resistors annotated with “R” and the inductors annotated with “L” represent parasitic line impedances. Power is auctioneered to ship loads through bus selectors that select which bus, port or starboard, energizes each load. Loads can draw power from either bus, but not both at the same time.

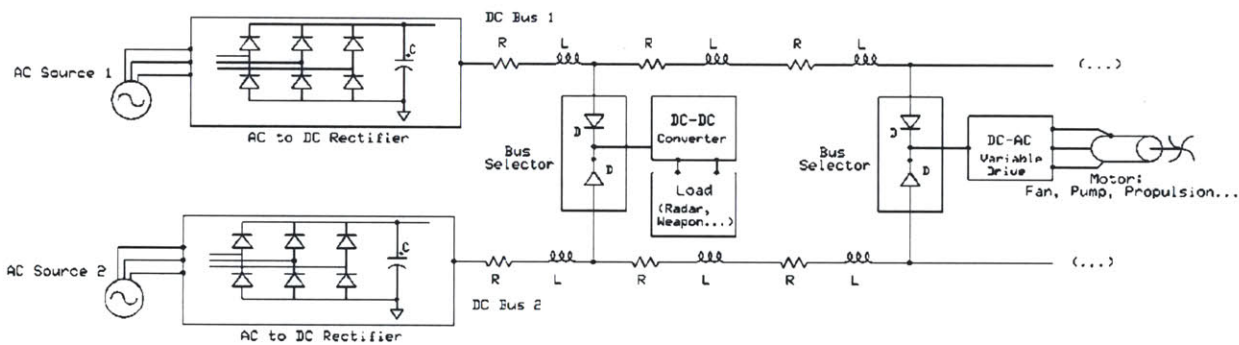


Figure 15: Nominal MVDC Distribution System (15)

The success of MVDC configuration, as shown above, relies heavily on the use of power electronic devices. DC-DC converters tied directly to the main distribution buses are used to transform the nominal bus voltage a current to level that will be used to supply such items as radars and weapons consoles. In addition to the DC-DC converters, DC-AC converters are used to create alternating voltage and current for loads like such as pump and fan motors and ultimately the electric propulsion drive. In this configuration, all the generated power is converted in to DC for distribution throughout the ship including all of the power for the ship propulsion drive.

### 3.3. Hardware Model

In years past, a test platform consisting of two 5000 watt synchronous generators was constructed to emulate a U.S. Navy DDG 51 FLT IIA class ship electric plant. This test platform

was originally built to evaluate the feasibility of improving the fault isolation capabilities of the MFM with NILM implementation. Since its construction it has been an invaluable asset for testing and evaluating various hypotheses concerning shipboard electric plants. To expand the simulations usefulness for the future, a DC distribution board construction was initiated for the purpose of evaluating testing and evaluating a number of research topics currently relating to MVDC power distribution.

### 3.3.1 Power Generation

The bench generator is a 4 pole, field wound synchronous generator. The stator is Y-connected with the neutral ungrounded and a rated voltage of 120 VRMS phase to neutral. The generators are used to supply AC power to the MVDC board



Figure 16: LEES Generator Setup and Specifications

The bench generator is being driven by two series connected 1.5 HP DC motors (120 Volts DC, 11.2 Amps, 4800 RPM).

Outlined in the figure below are the prime movers for the bench generator. The motors have a drive shaft that extends outward from either side of the motor housing which allows the motor to be centered between two driven loads. Rigidly coupling two motors together and connecting them in series electrically provides a rated capacity of 4 HP.

(This Page Intentionally Left Blank)



Figure 17: Coupled DC Drive Motors and Specifications

Providing power to the DC drive motors are Two XHR 1000 Watt Series programmable DC power supplies. The power supplies were placed in a parallel master-slave configuration to provide a rated output of 150 volts and 14 amps. These power supplies are controlled through a GUI interface on the computer that manipulates the output and thus the speed at which the motors spin the generators thereby controlling the bus frequency.



Figure 18: DC Motor Power Supplies

### 3.3.2 Variable Frequency Drive

In order to convert the DC power into AC for use by the propulsion drive, a variable frequency drive (VFD) is required. A variable frequency drive is a solid state electronic power conversion device. The usual design first converts AC input power to DC intermediate power using a rectifier or converter bridge. Here A full-wave, solid-state rectifier converts three-phase 60 Hz power from a standard 208, 460, 575 or higher utility supply to either fixed or adjustable DC voltage. The system may include transformers if higher supply voltages are used. Next the signal is passed to an inverter stage. In this stage electronic switches - power transistors or thyristors- switch the rectified DC on and off, and produce a current or voltage waveform at the

(This Page Intentionally Left Blank)

desired new frequency. The amount of distortion depends on the design of the inverter and filter. The switching frequency is determined by the control system. The circuit receives feedback information from the driven motor and adjusts the output voltage or frequency to the selected values. Usually the output voltage is regulated to produce a constant ratio of voltage to frequency (V/Hz). Controllers may incorporate many complex control functions.

For the MVDC simulation a Hitachi X200 VFD was chosen. This device has the ability to accept AC (230 V 3-phase) or Dc (300 V DC) and generate a 230 V 3-phase variable frequency (.5 – 400Hz) at the output.



Figure 19: Hitachi VFD

### 3.3.3 MVDC Board Description

The hardware model of the DC ZEDS board electrical is shown in the figure below. This board houses the ability to rectify and supply DC voltage to the load terminals. Solid State Relays are used to provide isolation and re-configurability of the distribution board. All loads are anticipated to be configured in a radial distribution configuration from one of the load centers attached to one of the two main bus lines. The MVDC board consisted of a control circuit, rectifiers, capacitors, relays and switches.

(This Page Intentionally Left Blank)



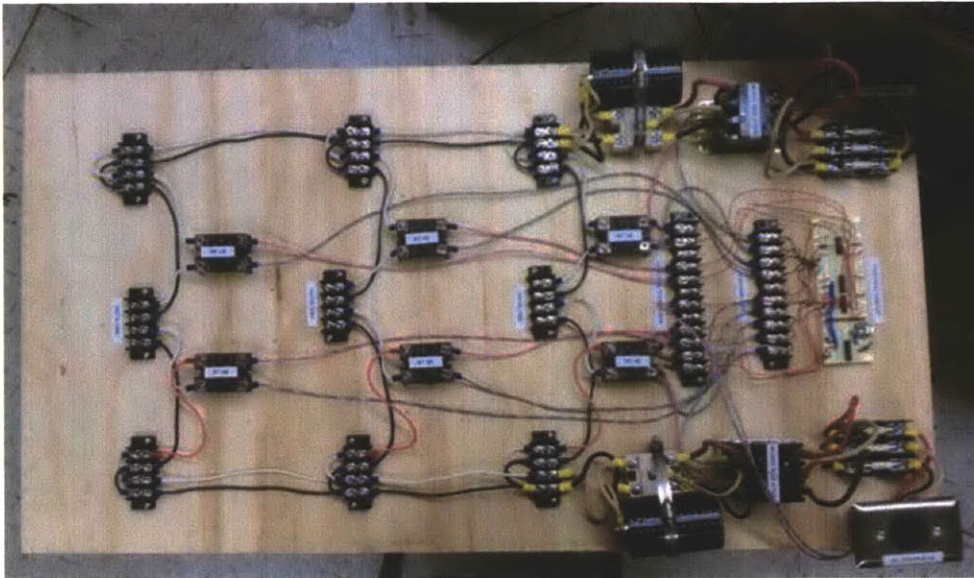


Figure 20: MVDC Hardware Model

### 3.2.3.1 Control Circuitry

The control circuitry for the MVDC boards uses a shift micro-controller to remotely control the contractors on the MVDC hardware model. The circuitry consists of one microcontroller (PIC16F628), one shift register (SL74HC595D) and one motor driver (L293D).

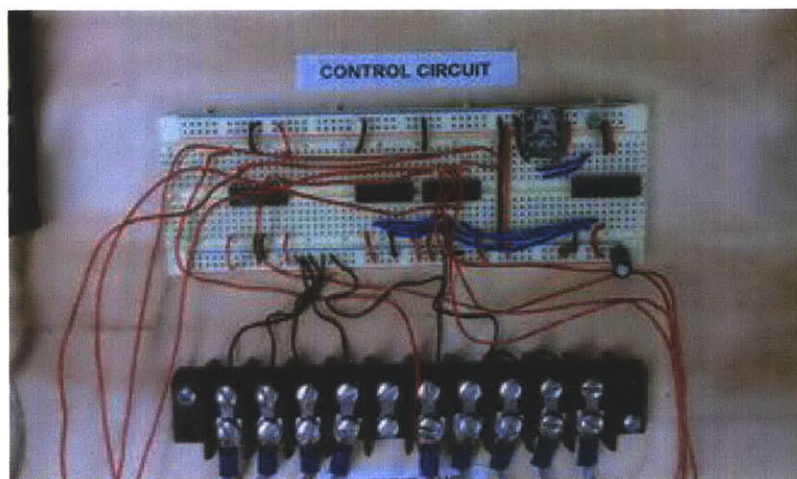


Figure 21: MVDC Board Control Circuitry

The PIC microcontroller is used to decode the signals that are generated from the MATLAB MVDC GUI. This device accepts inputs from the PC through a USB interface and converts the data into a binary string. The binary string that is generated by the PIC is stored in the shift

(This Page Intentionally Left Blank)

register. The shift store the data until additional user inputs are received or the device is de-energized. The motor driver is used to amplify the low voltage signal received from the shift register to a voltage sufficient enough to operate the relays.

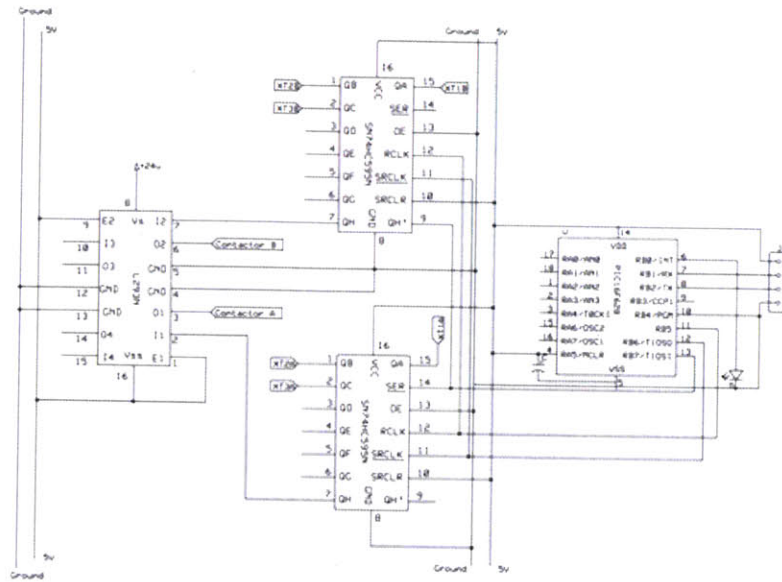


Figure 22: MVDC Board Control Circuit Schematic

### 3.2.3.2 Relays

For the MVDC board two types of relays were selected, two P31E contactors and six solid-state relays (SSRs). The two P31E contactors were used for isolating the AC power from the rectifier circuit. The P31E were required due to the 3-phase AC power coming from the generators. This type of relay relies on a zero crossing for operation. Due to the lack of a zero crossing when using DC, SSRs were used for the DC distribution section. The SSRs for DC loads do not require a zero crossing to shut. However, since the SSRs require much less control current to operate, the L293D chip is not required and all of the SSRs are controlled by the SL74HC595 chip output.

### 3.2.3.3 Rectification and Filtering

The heart of the MVDC board is in the AC to DC conversion. The AC to DC rectification for the MVDC board is provided via a bridge diode rectifier. Based on the break over voltage and the backing voltage required to “turn on” and “turn off” the diode a ripple will be present in the output waveform as shown in Figure 23. Application of the generator output to the bridge rectifier results in a rippled DC voltage. To smooth the output of the rectifier, a high voltage capacitor was added.

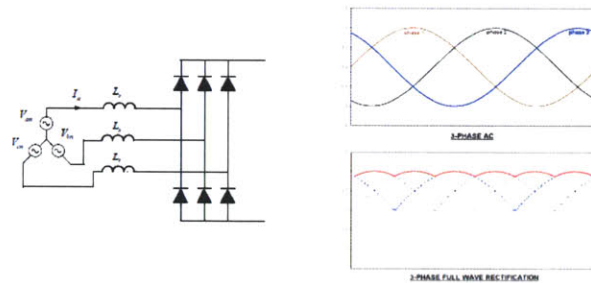


Figure 23: Bridge Rectifier Circuit and Waveforms

## **Chapter 4 Doubly-Fed Motor Propulsion Model**

### **4.1 Theory**

An alternative to deriving propulsion from an IPS without the need for converting propulsion power to DC is through a method discussed in (15). This method employs the use of a doubly-fed induction machine (DFM) instead of an induction or permanent magnet motor for propulsion. These DFM provides the unique ability to gradually bring up to speed high-inertia equipment and large loads smoothly and easily due to its ability to develop high starting torque at standstill while maintaining low inrush current. This type of machine is used in items such as electric power generating windmills, cranes, hoists, chippers and conveyors.

The DFM has windings on both stationary and rotating parts, where both windings transfer significant power between shaft and electrical system. The rotor windings are similar to those found on a typical DC armature. Electrical contact to the rotor windings is made through a set of slip rings. The stator and rotor windings can be operated shorted, energized with DC current, or driven with a fixed or variable frequency AC source. Several different combinations of winding excitation produce a useful motor. For example, with the rotor windings shorted and the stator driven with a fixed frequency AC source, the DFM operates in a manner essentially identical to a conventional squirrel-cage induction machine. Implementing such a machine within an IPS architecture has the potential to greatly reduce the quantity of power electronic devices required when compared to the MVDC design.

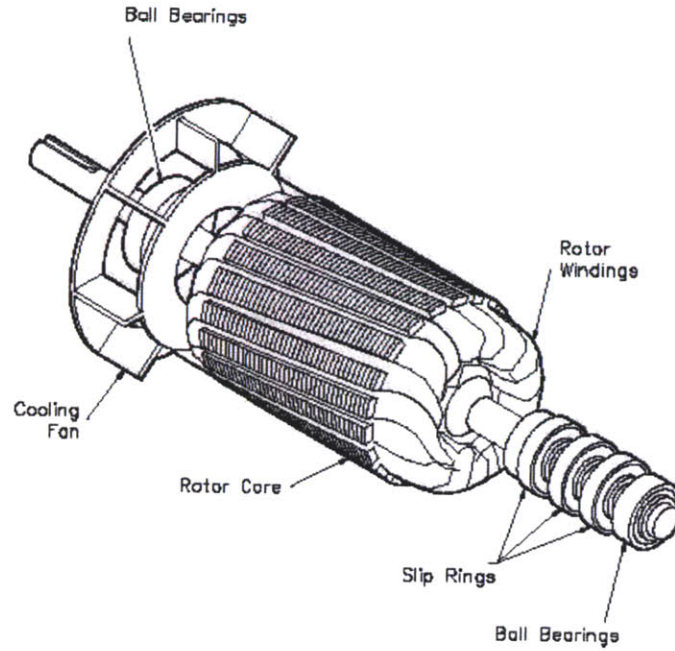


Figure 24: Nominal DFM Shaft Layout (18)

The wound-rotor machine has an external circuit connected via slip-rings as shown in Figure 25.

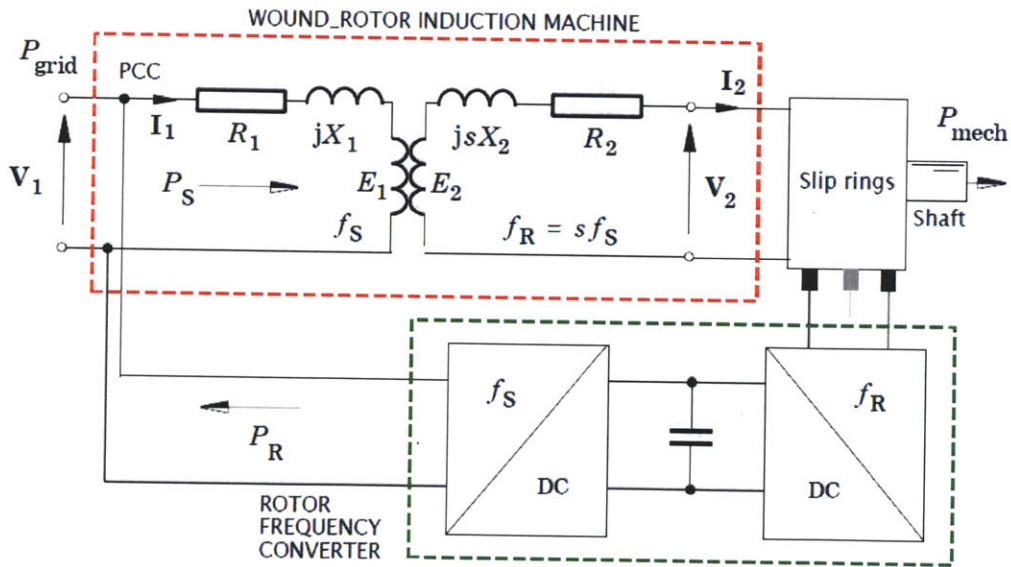


Figure 25: DFM Electric Circuit (16)

The following derivation is adapted from (16). To find the power balance for the machine we use the following equation:

$$P_{mech} = P_{gap}(1 - s) \quad (12)$$

where  $P_{mech}$  is the mechanical power (the sum of the shaft power and all the friction and windage power);  $s$  is the slip; and  $P_{gap}$  is the electromagnetic power crossing the air gap. In the wound-rotor machine, the power  $sP_{gap}$  is the sum of the dissipation  $I_2^2 R_2$  plus the real power in the external circuit. Therefore

$$sP_{gap} = P_{copper-loss} + P_r$$

where  $P_{copper-loss}$  is the “rotor copper loss” and  $P_r$  is the slip power flowing to the external rotor circuit. Using eq. 10, this can be re-written as

$$P_r = \frac{s}{1 - s} P_{mech} + P_{copper-loss}$$

In large machines  $P_{copper-loss}$  is typically small, and it is intended that most of the slip power passes out to the external rotor circuit.

#### 4.2 DFM Propulsion System Operation

At least two different operating configurations of the DFM are of concern for a ship propulsion application. In the first operating configuration, the DFM stator is energized with DC excitation. During this mode the stator serves as an electromagnet, creating a fixed set of north and south magnetic poles in the fixed, non-rotating reference frame of the ship. The rotor is energized with variable frequency AC waveforms from a power electronic drive. In this configuration, the magnetic field patterns created by the stator and rotor with power electronic drive are much like a classic, brushed, wound-field DC motor. Although the DFM has no mechanical commutator, the variable speed drive for the rotor will serve as an “electronic commutator,” and the machine is capable of producing torque in this configuration. The DC power used to energize the stator is likely to be negligible, limited to the ohmic losses on the stator, however, considerable power, whether AC or DC, will be needed to energize the variable frequency power electronics associated with the rotor (15).

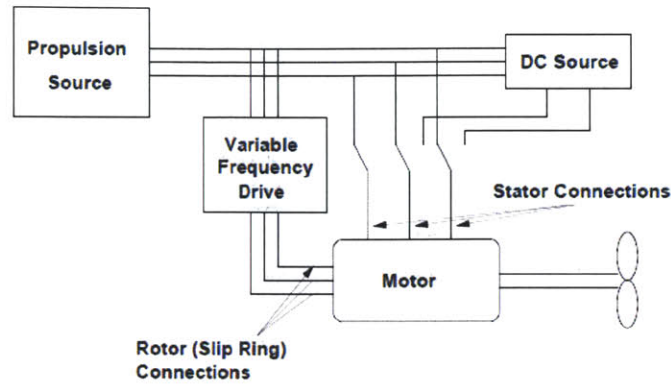


Figure 26: Simplified DFM Operation Schematic (17)

A threshold in operating condition is reached in this mode of operation when the frequency of the AC waveform on the rotor the same frequency as the synchronous or utility electric frequency, assumed fixed, on the ship. At this point, the machine could be operated in one of two configurations, either of which will produce identical torque and speed. The DFM could be operated with DC current on the stator and AC created by the rotor power electronics at synchronous utility frequency on the rotor. Alternatively, at this synchronous shaft speed, the rotor could be energized by a DC current, and the stator could be powered by the fixed-frequency AC bus that is conventionally available on most ships. This alternative configuration creates a magnetic field pattern typically associated with a “brushless” DC or permanent magnet synchronous machine. If the DFM operates with fixed-frequency AC on the stator and DC current (zero frequency) on the rotor, it runs at synchronous speed. Rotor power drops to just the ohmic dissipation associated with running the rotor windings at DC. This is likely a negligible amount of power.

If required, the speed of the DFM can be further increased in a second operating configuration. This arrangement requires the stator to be connected to the fixed frequency AC source the rotor energized from the power electronic AC drive. Rotor power, increasing from zero at synchronous shaft speed, is again delivered to the rotor from the variable frequency power electronic drive, accelerating the rotor past synchronous speed. The machine operates with negative slip. Significant power is also delivered to the machine stator from the fixed-frequency AC utility source.



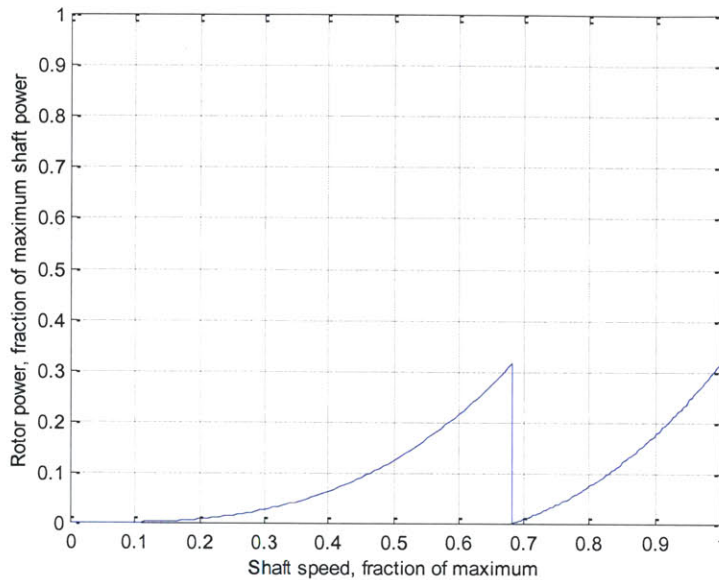


Figure 27: Operating Curve for DFM (17)

In summary, employing the use of a DFM has the potential to significantly reduce the amount of DC power required and thus the quantity of power electronic devices when compared to a conventional induction or permanent magnet motor IPS configuration. With the stator energized by DC current, the rotor is energized by the power electronics, gradually increasing in power, electrical frequency, and shaft speed to any required operating frequency below synchronous shaft speed. At this “cutover” or synchronous shaft speed, the rotor electrical power reaches its peak, and the machine is transitioned to the second operating mode. The stator is disconnected from the DC supply, allowing enough time, likely tens of milliseconds, for the DC current to decay, and then connected to the ship’s utility AC supply. Once the AC supply is connected to the stator, the rotor can be excited, most likely by power electronics configured to look like an adjustable frequency current source that will inject current to “push” against the rotating flux wave created by the stator. The rotor power electronics can be limited to a peak power level equal to the needed rotor power at the synchronous shaft speed. The peak shaft speed, which exceeds synchronous shaft speed, will occur in the second operating mode as the rotor accelerates past synchronous speed. The rotor electronics eventually reach peak operating power for a second time. Equating the rotor power requirement at the end of the first operating region at

(This Page Intentionally Left Blank)

synchronous speed with the level at the end of the second operating region at full shaft speed permits determination of the power rating requirements for the rotor electronics.

## 4.2 Hardware Model

To facilitate the examination of the DFM propulsion theory, a scaled hardware model was constructed. This hardware model consists of two 2 HP DFM, one permanent magnet motor and two ABB VFDs. The components were selected to provide an adequate power level for proving the DFM propulsion theory, yet small enough to be housed within the LEES lab without the need for a great amount of real estate. It was also desired that the hardware model incorporate the ability to be repositioned to allow for testing from various electrical power sources contained within the LEES lab.

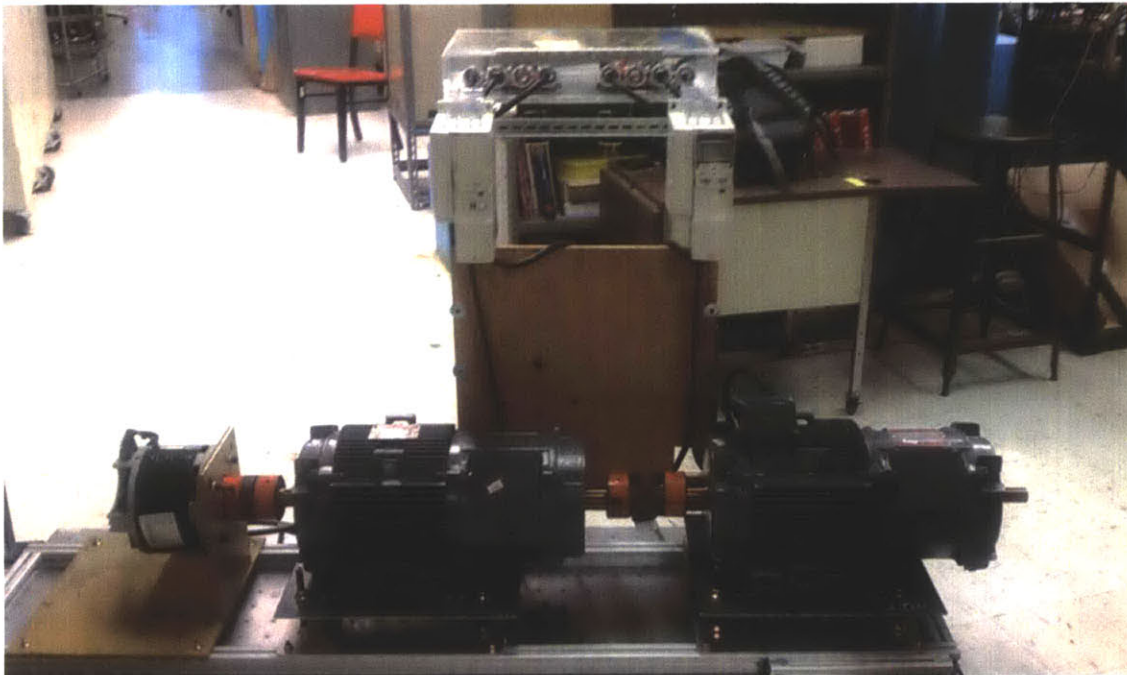


Figure 28: DFM Simulation Cart

### 4.2.1 Doubly-Fed Motors

Obtaining a reasonably sized three phase AC generator was the starting point for creating the propulsion hardware model. Ultimately two DFM were selected that provided the desired capabilities in a package that could easily be transported through the lab. The DFMs selected are rated for at 2 HP, 1200 RPM and can be operated from either a 230V or 460V 3-phase source.

(This Page Intentionally Left Blank)

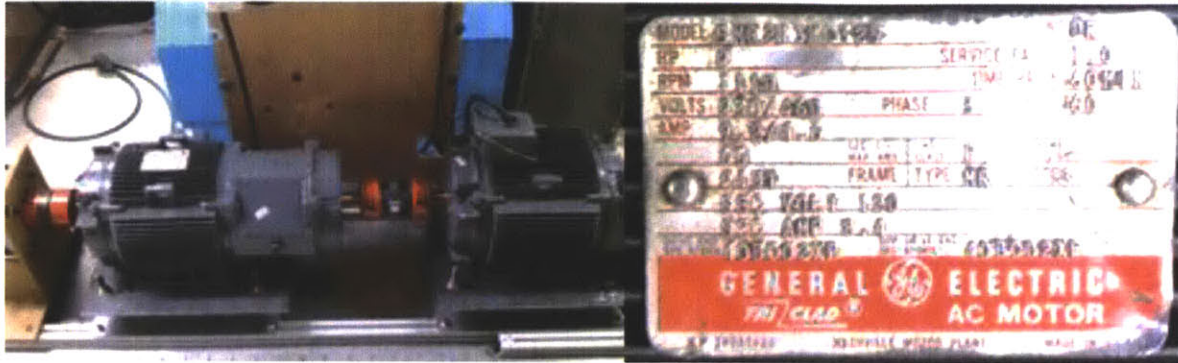


Figure 29: DFM and Nameplate

#### 4.2.2 Variable Frequency Drives

The VFDs that were used for this simulation are similar in operation to those that were selected for the MVDC board simulation. For this simulation ABB ACS 355 VFDs were chosen due to their ability to operate at low frequencies potentially eliminating the need for switching between DC and AC power sources and their interface modularity. The ABB ACS 355 VFD not only provides the user the ability to operate VFD parameters from the front control panel, but provides an interface such that the VFD can be controlled directly from a PC via an RS-232 port.

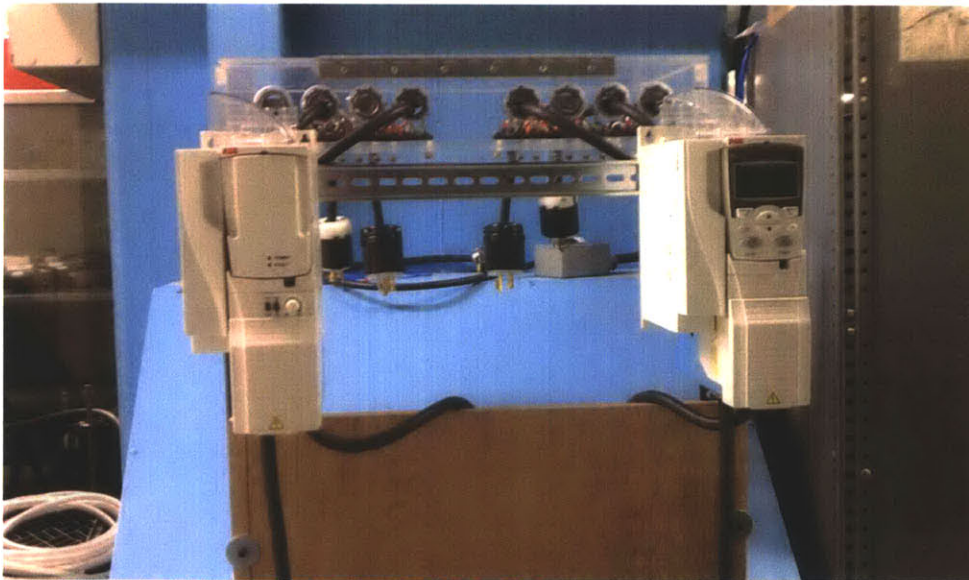


Figure 30: ABB ACS 355 VFDs

The primary method of control is through the use of the advanced control panel. The advanced control panel provides the user access to various configurable parameters within the VFD. These parameters allow the user to configure such items as volts/Hz ratios as well as frequency ramp rates. In addition to the advanced control panel the VFD can be operated from a

(This Page Intentionally Left Blank)

PC through the Drive Windows Light™ software distributed by ABB. The Drive Windows Light™ software allows users to monitor a drive's parameters and signals, and even to control the drive from a PC. The tool also has an I/O mapping table for quickly viewing the drive's input and output configuration. Currently Drive Windows Light™ is installed on the PC used to operate the MVDC board. The final method for interfacing with the VFD is through the use of a potentiometer. This is the simplest interface method. This interface provides the user the ability to adjust the frequency and direction of rotation. When using this control method, the operator is not provided a visual indication of the frequency, thus alternate methods have to be employed if a visual indication of frequency is required.

#### 4.2.3 Permanent Magnet Motor

The use of the permanent magnet motor is to supply the DFM with a backing torque to provide loading once the propulsion motors are operating. This was done such that the hardware model could produce results that more closely simulate those that would be obtained if the field. Several loading condition can easily be implemented with the DC motor through the use of a control circuit. A control circuit can be used to manipulate the duty cycle of the DC motor and thus ultimately adjusting the average load seen by the DFM. The control circuit to conduct this operation was not constructed as part of this thesis.

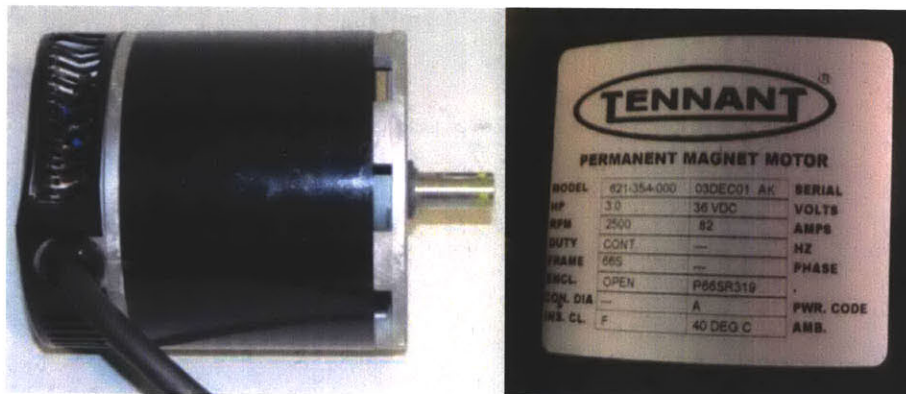


Figure 31: Permanent Magnet DC Motor

#### 4.2.3 Motor Cart

To allow for portability of the DFM hardware model it was decided to construct the model on a portable platform. The platform that was chosen for this duty was an optical table.

(This Page Intentionally Left Blank)



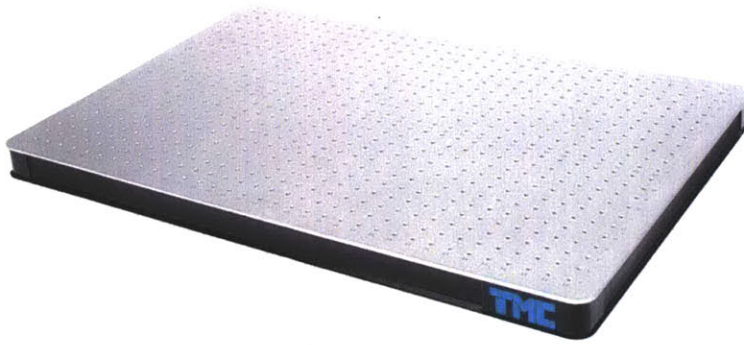


Figure 32: Optical Table Base

The optical table not only provided the capability to install wheels for portability, it also provided the structural integrity to support the DFM and ensured that the mounting hardware was perfectly aligned. 80/20 box aluminum channel tubing was attached along the perimeter of the optical table. This provided base in which the DFM could be mounted that was independent of the mounting locations provided by the optical table. Additionally, the use of the aluminum tubing minimized the weight of the overall design.



Figure 33: 80/20 Box Tubing

The box tubing was attached to the optical board through the use of T-channel locking mechanisms. These devices are used to interface with the slots on the box tubing and allow the joining of the box tubing to other assemblies.

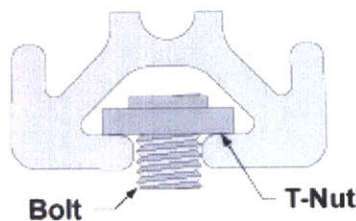


Figure 34: T-Channel Locking Mechanism

(This Page Intentionally Left Blank)

While the same T-channel locks could be utilized for the installation of the motors, it was desired to incorporate flexibility into the motor mount to allow for the installation of several different motor mounting configurations. To provide this capability, an adjustable mounts was constructed of aluminum and steel.

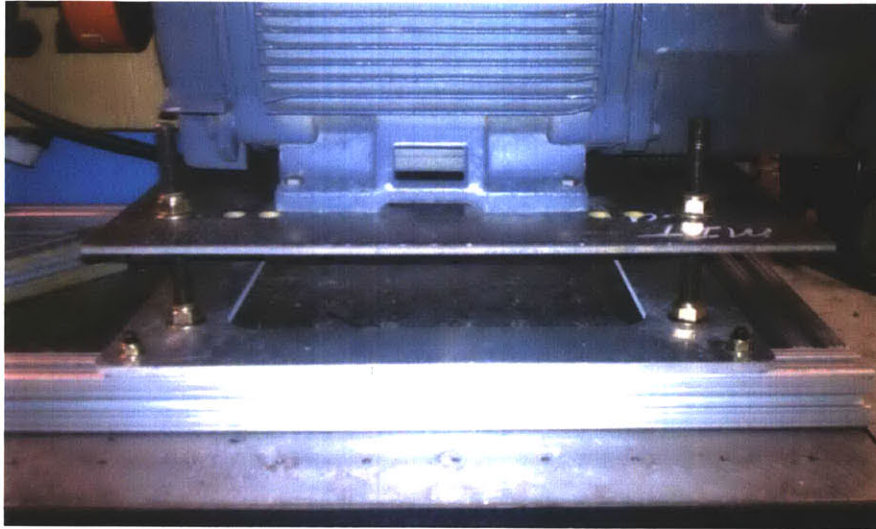
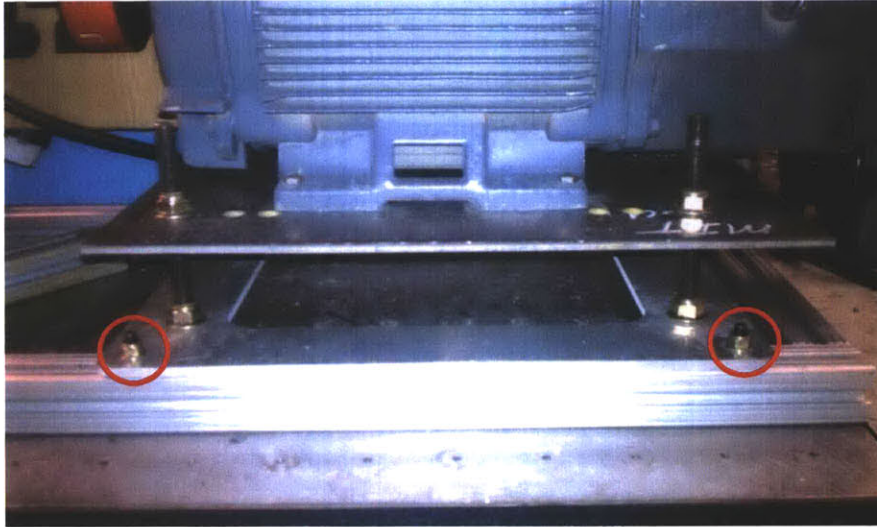


Figure 35: Motor Mounting Hardware

The base of the motor mount was constructed of aluminum while the upper section which bears the load of the motors was constructed of steel. This mix of materials was selected to save weight as well as provide the structural strength and rigidity necessary to secure the motors.

The short mounting bolts, highlighted in red, were used to mount the aluminum guide base to the 80/20 channel tubing. A total of four guide bolts were used at the corners of the guide base. Loosening the guide base bolts allows for the entire motor mount to translate the length of the optical board. This configuration allows for easy coupling and decoupling of motors. With the guide bolts securely fastened, the motor is locked in place. Nuts with nylon inserts were used to ensure that the nuts will remain tight once secured.

(This Page Intentionally Left Blank)



**Figure 36: Motor Base Guide Bolts**

Attached to the guide base is the motor mount. This is attached through the use of threaded shaft and a unique configuration of nuts and washers to allow provide maximum flexibility. The steel motor mounting base encompasses several penetrations to allow for a wide variety of NEMA motor frame installations.

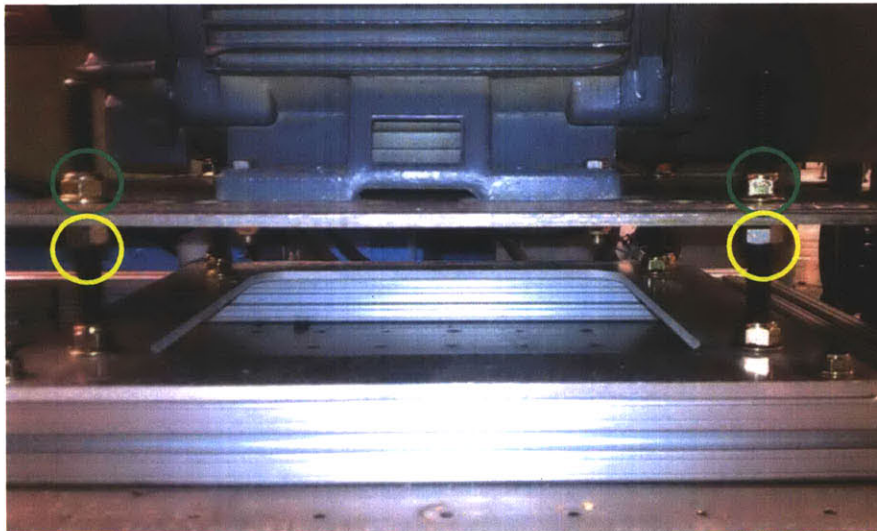


**Figure 37: Motor Base Adjustment Bolts**

The configuration of nuts and bolts allow for the raising and lowering of the motor mount platform to ensure motor shafts are properly aligned. To raise the motor platform, first loosen the bolts highlighted in green. Next operate the nuts highlighted in yellow, using an adjustable wrench or  $\frac{3}{4}$  inch open box wrench, in the counter-clockwise direction. This operation should

raise the platform. Conduct this operation for the remaining three corners. Once the operations is complete, secure the platform by re-tightening the nuts highlighted in green and verify that the platform is level using a torpedo level or by measuring the platform height at all corners. To lower the motors, conduct a similar operation, but manipulate the nuts highlighted in yellow in the clockwise direction.

## **Chapter 5 Conclusion**

### **5.1 Speed Harmonic Future work**

The synchronous speed harmonic oscillation experiments conducted accomplished the purpose of demonstrating that the NILM can indeed be used to monitor vibrations within rotating machinery. It has been shown that in a controlled environment the speed harmonic oscillations monitored by the NILM can be directly related to the observed reading of a vibration meter. While the sole use of NILM as a replacement for vibration monitoring of equipment shows great potential, there are still several physical aspects which require further analysis. Areas of particular interest are how to compensate for the harmonic frequency shift due to the voltage droop and harmonic interference that will be present due to cycling loads. New algorithms and motoring techniques are currently being explored.

### **5.2 MVDC Future Work**

The MVDC hardware model constructed provides a platform for which new theories and algorithms relating to MVDC propulsion can be analyzed. Future work for this project includes the continuous updating of the test platform as additional information is obtained regarding the final configuration, protection capabilities and limitations. The closer that the hardware model can portray reality, the more useful the results in the lab environment become.

### **5.3 DFM Future work**

The DFM hardware model constructed provides a reference for evaluating the propulsion concept in steady state. To determine the transient effects on the design a method to seamlessly alternate between applying AC or DC power to both the rotor and stator need to be developed. The development of this control system will allow for better compare and contrast with other proposed electric propulsion methods. Furthermore, there are many open questions concerning the feasibility of a practical DFM. Slip rings are required for operating the machine. The rating of these slip rings is likely to be larger than, but not necessarily substantially larger than, slip rings currently employed on utility turbo-generators. The geometry and modularization of the DFM for shipboard application both need further study.

## Works Cited

1. Reduction Of Total Ownership Costs. [Online] August 24, 2010. [Cited: January 23, 2011.] <http://ve.ida.org/rtoc/rtoc.html>.
2. *R-TOC in DoD Systems*. **Dr. Spiros Pallas, Principal Deputy, OSD/Defense Systems**. 2002.
3. **Change, The Observe: Special Edition - NAVSEA Agenda for**. *From The Front Office*.
4. NAVY. *SBIR FY08.3 PROPOSAL SUBMISSION INSTRUCTIONS*. [Online] [Cited: November 12, 2010.] <http://www.acq.osd.mil/osbp/sbir/solicitations/sbir083/navy083.htm>.
5. **Lee, K.** *Electric load information system based on non-intrusive power monitoring*. Cambridge : Massachusetts Institute of Technology, 2003.
6. *Coast Guard RCM/CBM Initiative*. **Linton, E.** Birmingham, AL : Department of Defense Maintenance, 2005.
7. *Failure Identification of Offshore Induction Motor*. **W. T. Thomson, R. A. Leonard, A. J. Milne, and J. Penman**. 1, s.l. : Reliability Engineering, 1984, Vol. 9.
8. *Transient event detection in spectral envelope estimates for nonintrusive load monitoring*. **Leeb, S.B., Shaw, S.R. and Kirtley, J.L., Jr.** 1995, IEEE Transactions, pp. 1200-1210.
9. **Cox, R. W.** *Minimally intrusive strategies for fault detection and energy monitoring*. Cambridge, MA : MIT, August 2006.
10. *Current Signature Analysis to Detect Induction Motor Faults*. **Fenger, William T. Thomson and Mark**. July/August 200, s.l. : IEEE Industry Applications Magazine, 2001.
11. *Motor bearing Damage Detection Using stator current*. **Habetler, R. R. Schoen and T. G.** 6, s.l. : IEEE Transaction, 1995, Vol. 31.
12. *Methods of Motor Current*. **Stein, G. B. Kliman and J.** 5, s.l. : Electric Machines and Power Systems, 1992, Vol. 20.
13. **Doerry, Captain Norbert H.** *Next Generation Integrated Power System for the Future Fleet*.
14. **Doerry, CAPT Norbert.** *Next Generation Integrated Power System: NGIPS technology development roadmap*. Washington, D.C. : Naval Sea Systems Command, November 2007.
15. *How Much DC Power is Necessary*. **Dr. Steven B. Leeb, Dr. James L. Kirtley, Jr. et. al.** 2, s.l. : Naval Engineers Journal, 2010, Vol. 122.
16. *Using the Non-Intrusive Load Monitor for Shipboard Supervisory Control*. **Cox, R.W., et al., et al.** s.l. : IEEE, 2007. Electric Ship Technologies Symposium. pp. 523-530.



17. *Current signature analysis to detect induction motor faults*. **Thomson, W.T. and Fenger, M.** 2001, Industry Applications Magazine, pp. 26-34.
18. *A review of induction motors signature analysis as a medium for faults detection*. **El Hachemi Benbouzid, M.** 2000, Industrial Electronics, IEEE Transactions, pp. 984-993.
19. **Leeb, S.** *A Conjoint Pattern Recognition Approach to Nonintrusive Load Monitoring*. Cambridge : Massachusetts Institute of Technology, 2003.
20. **Douglas, K.** *Shipboard Aggregate Power Monitoring*. Cambridge : Massachusetts Institute of Technology, 2008.
21. **Leghorn, J.** *Modeling for Ship Power Emulation*. Cambridge : Massachusetts Institute of Technology, 2009.
22. *Detection of rotor slot and other eccentricity related harmonics in a three phase induction motor with different rotor cages*. **Nandi, S., Ahmed, S. and Toliyat, H.A.** 2001, IEEE Transactions, pp. 253-260.
23. *Induction motors' faults detection and localization using stator current advanced signal processing techniques*. **Benbouzid, M.E.H., Vieira, M. and Theys, C.** 1999, IEEE Transactions, pp. 14-22.
24. *Case histories of current signature analysis to detect faults in induction motor drives*. **Thomson, W.T. and Fenger, M.** s.l. : IEEE International, 2003. Electric Machines and Drives Conference. pp. 1-4.
25. *Rotor fault diagnosis based on current signatures in squirrel-cage induction motor*. **Hammadi, K.J., Ishak, D. and Salah, W.** 2010, Electronic Devices, Systems and Applications (ICEDSA), pp. 11-14.
26. *Detection of Motor Bearing Outer Raceway Defect by Wavelet Packet Transformed Motor Current Signature Analysis*. **Lau, E.C.C. and Ngan, H.W.** 2010, IEEE Transactions, pp. 2683-2690.
27. **Bowman, Frank L.** *An Integrated Electric Power System: the Next Step*. [Online] [Cited: October 30, 2010.] [http://www.navy.mil/navydata/cno/n87/usw/issue\\_9/power\\_system.html](http://www.navy.mil/navydata/cno/n87/usw/issue_9/power_system.html).
28. *Method for detection of broken bars in induction motors*. **Dobrodeyev, P.N., et al., et al.** 2000, IEEE Transactions, pp. 3608-3610.
29. *Induction motors' faults detection and localization using stator current advanced signal processing techniques*. **Benbouzid, M.E.H., Vieira, M. and Theys, C.** 1999, IEEE Transactions, pp. 14-22.

(This Page Intentionally Left Blank)

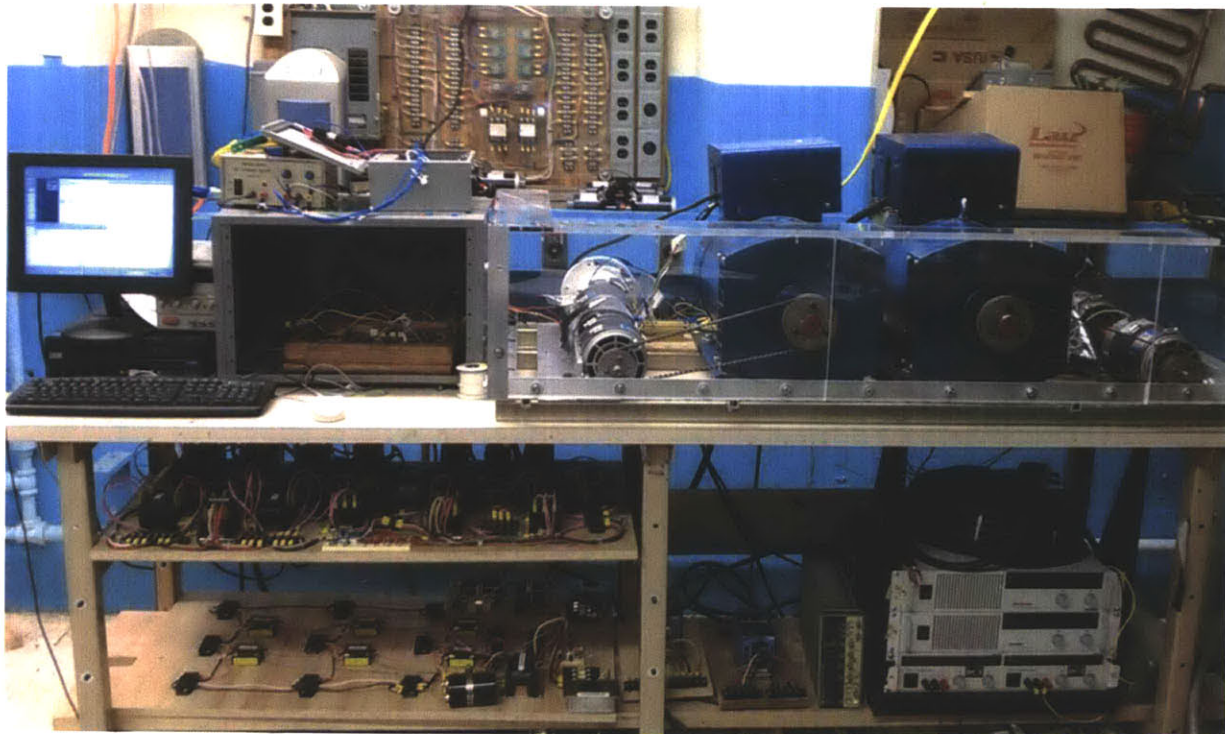
## APPENDIX A

### Generator and MVDC Board Operating Instructions

#### Tools Required:

1/8 inch hex key  
17mm socket  
Ratchet  
Flathead Screwdriver  
Multimeter

#### Overall Architecture

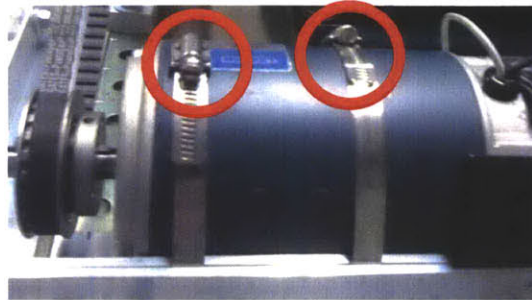


#### Initial Conditions:

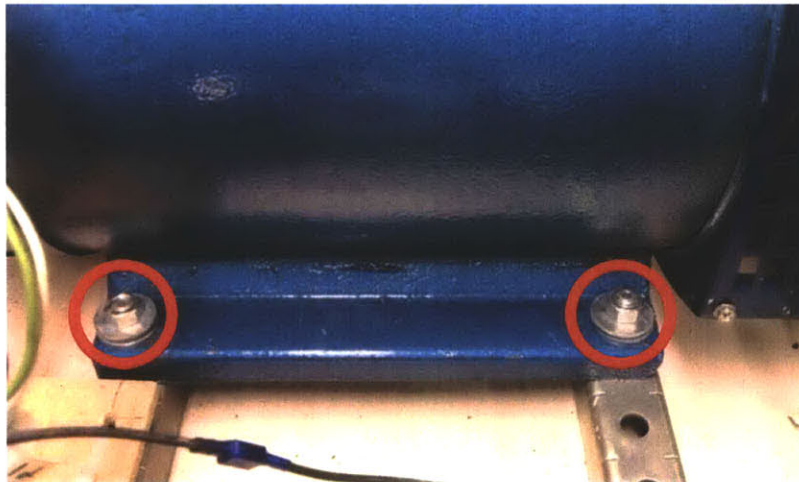
1. Inspect all cabling to verify integrity. Ensure that all conductors are intact and that there is no chaffing, a break or damage to the insulation and/or current carrying conductors. In addition verify the following electrical connections to power supplies and to the generator are sufficiently taught (not too tight not too loose):
  - a. Generator output terminals
  - b. DC Motor fan power supply leads
  - c. Leads is connected between the power supplies labeled DCM 1 and 2 to the DC Motors labeled DCM 1 and 2

(This Page Intentionally Left Blank)

- a. Leads connected between the DC1 and DC2 power supplies and the Field Windings of Generator 1 and 2
3. Inspect the four (4) DC drive motors are firmly mounted to the base frame and that the holding strap is adequately tightened to prevent movement during operation. (2 straps per DC motor)

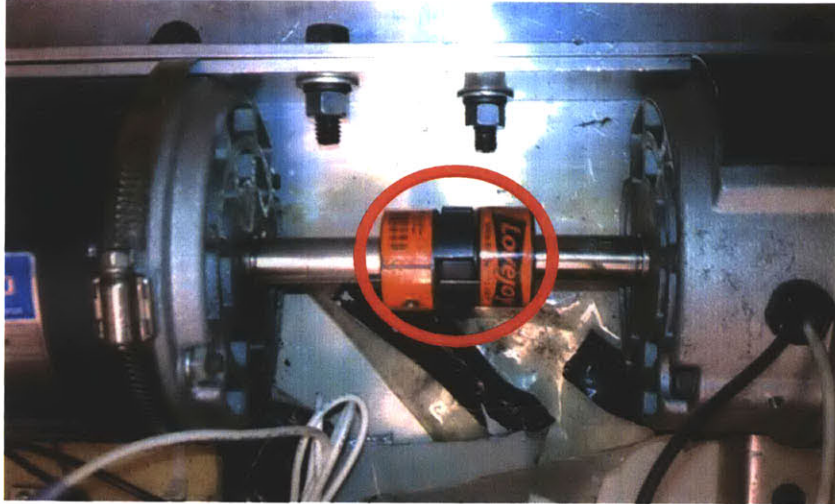


4. Verify that the generator mounting bolts are sufficiently tight to prevent movement during operation. (total of 4 per generator)

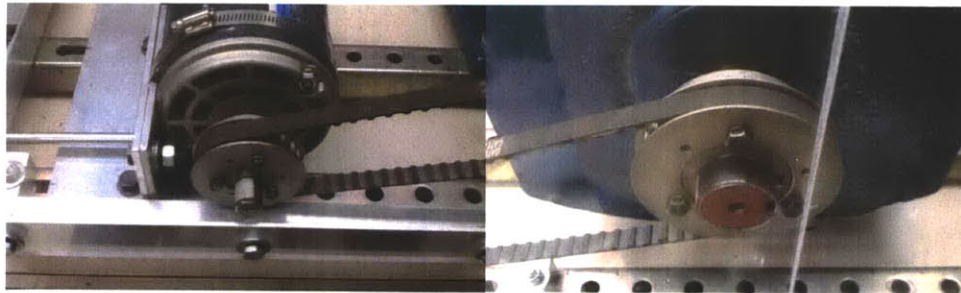


5. Inspect the shaft coupling between the DC motors ensuring that the set screws are tight and that each spider coupling is making sufficient contact with the spider. There should be less than 1/8<sup>th</sup> inch between the coupling hub and the spider. You should not be able to see light through the spider coupling from the opposite side. If coupling is outside of specification, loosen the holding straps and adjust motor until within spec.

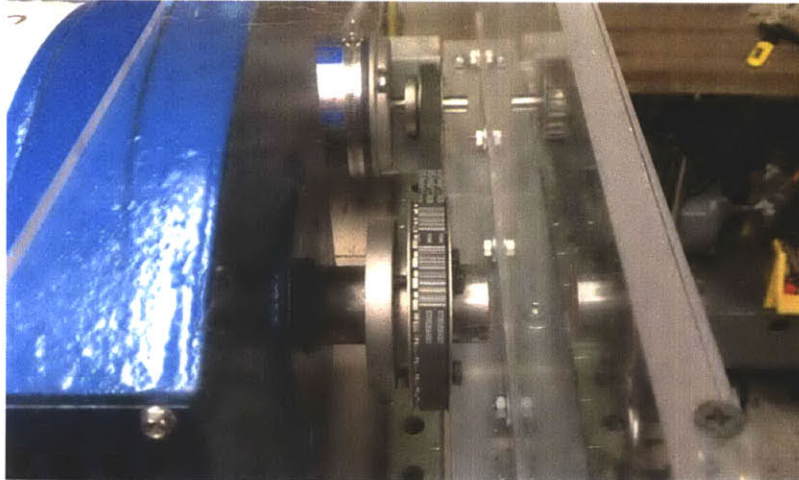
(This Page Intentionally Left Blank)



6. Inspect the DC motor belt drive sprocket and generator sprocket for integrity, tightness and alignment.



7. Using a large T-square placed along the edge of the Plexiglas enclosure provides an adequate line of sight for verifying belt alignment.

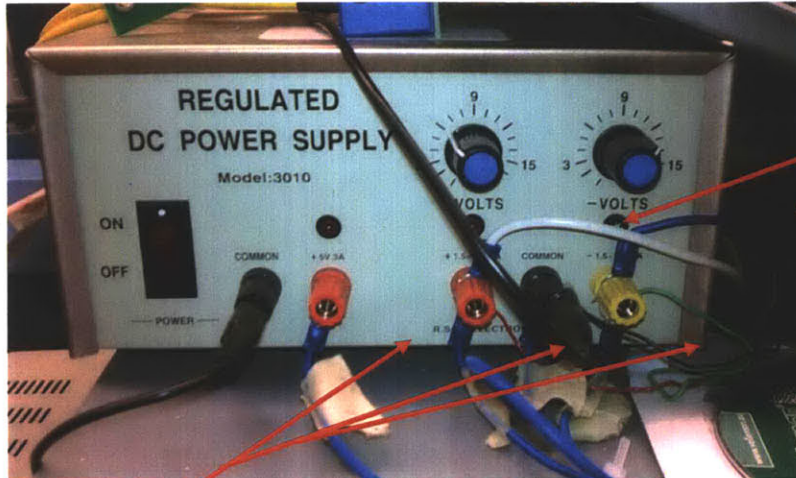


8. Inspect the Plexiglas enclosure and verify that it is free of all tools and debris.
9. Verify both motors and generators rotate freely.
10. Verify that there is adequate power to all supporting equipment, i.e. computer, power supplies, etc.

(This Page Intentionally Left Blank)



**Power Supply Verification:**



DC Motor Fan Power Supply

Figure 38: Fan/NILM Power Supply (PS1)

NILM Power Supply

**Power Supply 1 (PS1) Checks:**

1. Verify +12 V (white wire) and -12 V (blue wire) to both DC Motor fans.
2. Verify +5 V; ±12 V and Common (blue wires with tape labels) are connected to the NILM box.
3. Verify power supply two (PS2) is set for 24 volts and 3 Amperes. This supplies power to the relay circuitry. Connect +24V to the AC and/or DC ZEDS board the pink and the grey wire leading to the AC ZEDS Board and/or DC ZEDS board to the ground.



Figure 39: Relay Power Supply (PS2)

(This Page Intentionally Left Blank)

## Startup Procedure

1. Open the Generator Control GUI on the desktop: GeneratorController.exe. The file is located on the desktop of the computer adjacent to the generator setup or in the following directory: C:\Program Files\Nerdjack\GeneratorController.exe



The following GUI should be displayed on the computer monitor after the program is executed:

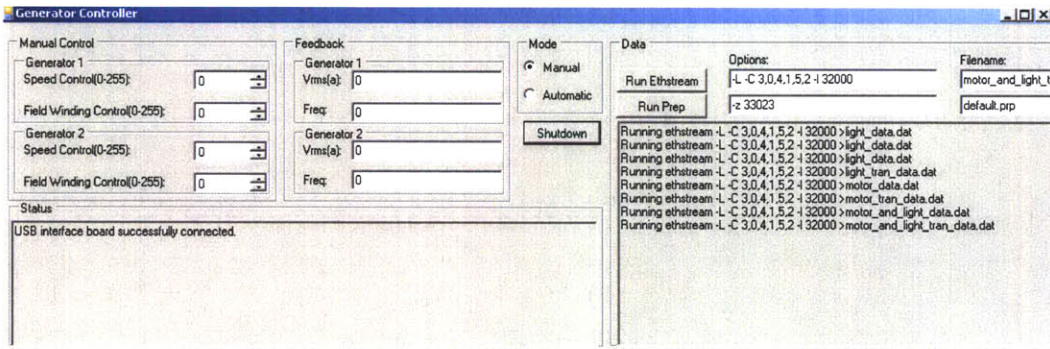


Figure 40: Generator Controller GUI

2. Turn on the field winding and DC motor power supplies (4 power switches total). The power supplies will NOT respond to the inputs from the front panels. All power supply regulation is handled by through the Generator Controller GUI.



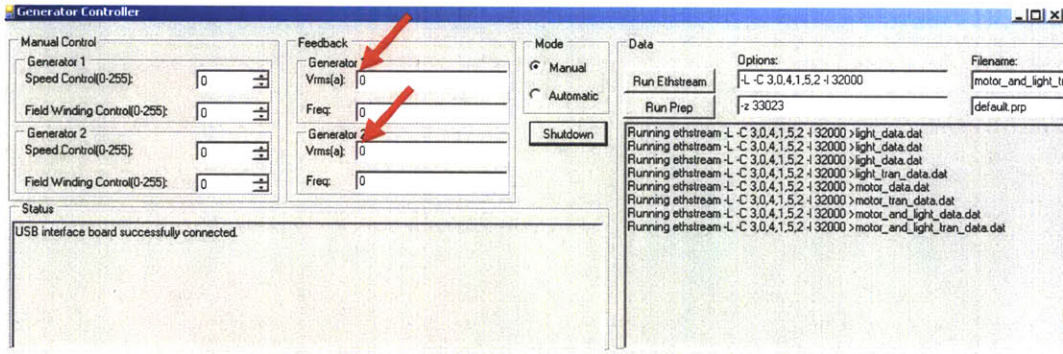
Figure 41: DC Motor and Field Winding Power Supplies

(This Page Intentionally Left Blank)

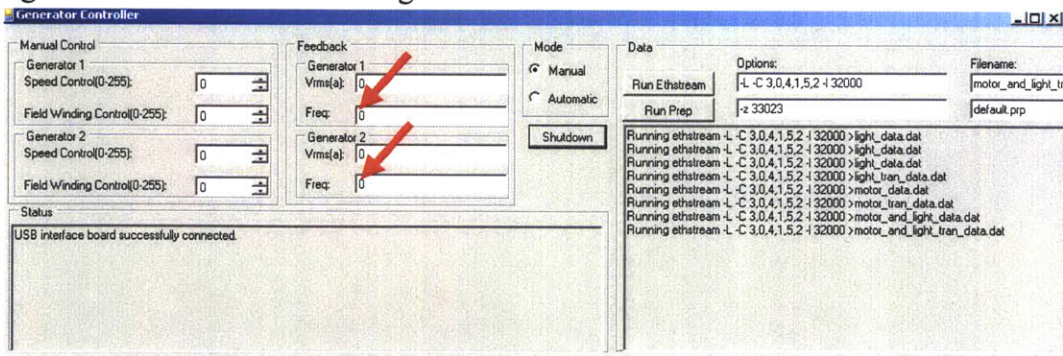
3. Energize PS1 and PS 2.



4. Slowly increase the speed control indicator on the GUI by for depressing the up arrow the desired generator to be used for testing to verify rotation. DC motor and generator should rotate freely. **If the motor or generator does not rotate, secure the setup and re-verify the lineup.** Once proper operation of both DC motor(s) and generator(s) depress the shutdown pushbutton on the generator controller GUI. Both motors should slow and stop.



5. Verify positive control of the Field Windings by depressing the up arrow for the field winding control. Verify the DC power supply corresponding to the generator you are trying to control increases in voltage and current.



(This Page Intentionally Left Blank)

- Open MATLAB and execute the DC ZEDS MATLAB GUI DC\_zeds\_gui\_v3.m. Script can also be located in Appendix C. To execute the script depress the green arrow. Upon execution the following figure should display.

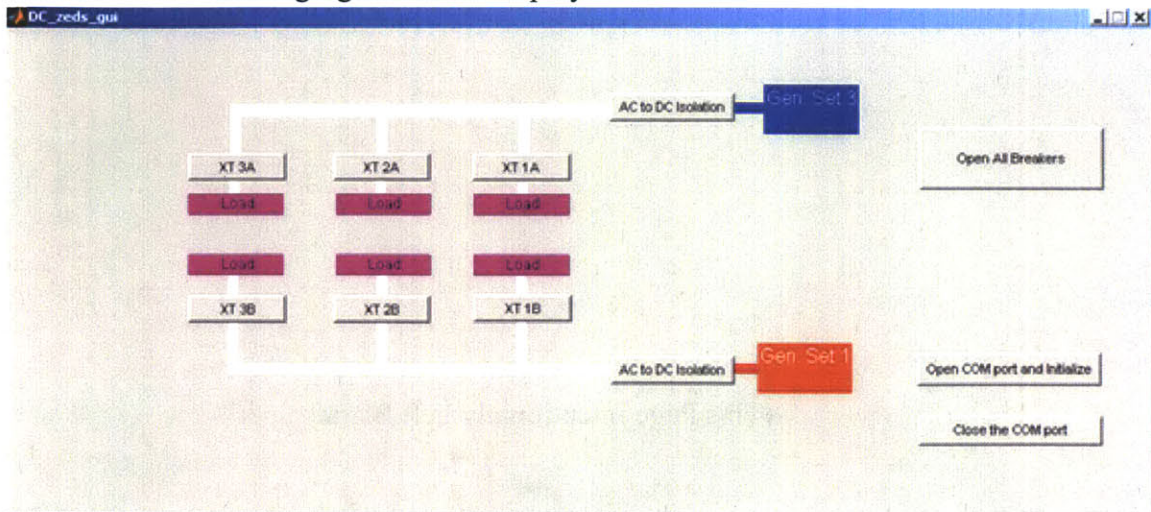
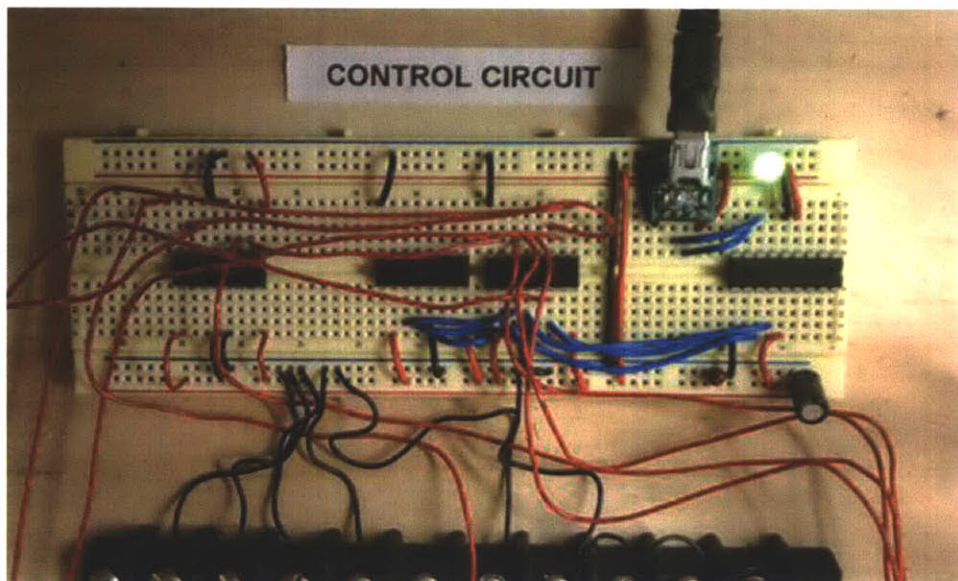


Figure 42: MATLAB DC ZEDS GUI

- Verify that the mini-USB form the PC is connected to the control circuit of the MVDC board and that the LED illuminates.



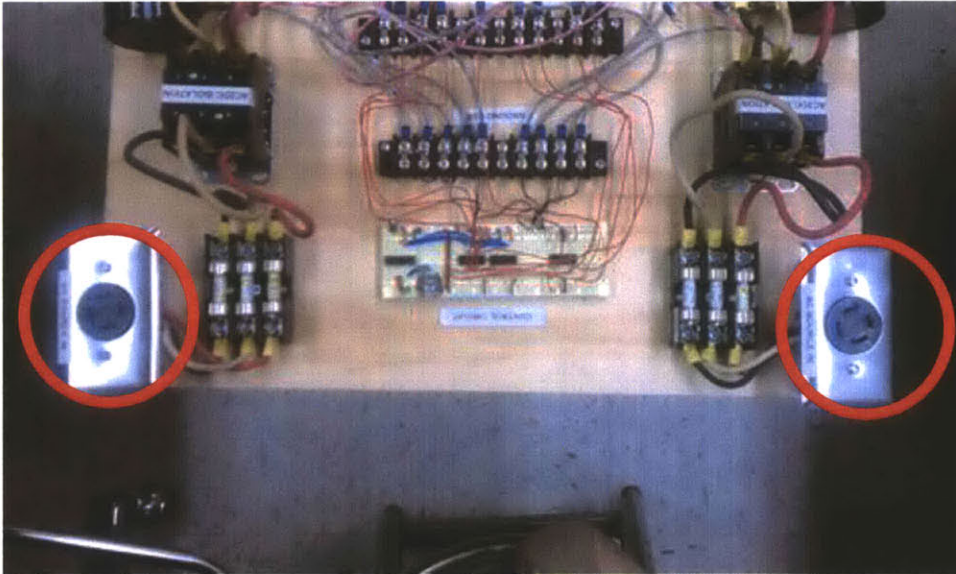
- Depress the “Open COM port and initialize” push button. Cycle each of the relays on the GUI to verify that the computer is properly communicating with the MVDC board. To verify the XT relay operation, visually inspect the relays red indicator light(s). There will not be a “click” when the relay is energized, the red light on the relay will illuminate when the relay is shut and de-energize when the relay is open. The AC to DC isolation relays will “click” during opening and closing.
- The setup is now ready for operation.

(This Page Intentionally Left Blank)



## Operating the Motor Setup

1. Locate the AC inputs on the MVDC Board.



2. To supply power from the generator(s) to the MVDC board plug the supply cable from the generator into one or both of the receptacles on the MVDC board.



3. Startup the generator setup in accordance with the previous setting. Increase dc motor speed until the desired AC frequency is achieved. The speed of the DC motors will have to be readjusted as the generators are loaded in order to maintain a constant AC supply frequency.
4. Slowly increase the field winding supply until the desired voltage is achieved.
5. Shut or open the relays using the MATLAB script to supply power to the buses.
6. Loads can be connected to the MVDC board through the load terminals. Verify to the rating to ensure that it is capable of handling  $\geq 300V_{dc}$  at the supply terminals.

(This Page Intentionally Left Blank)

## APPENDIX B

### Doubly-Fed Induction Machine Operating Manual

#### Tools Required:

3/16 inch hex key

1/2 inch wrench

3/4 inch wrench

Flathead Screwdriver

Multimeter

#### Overall Architecture

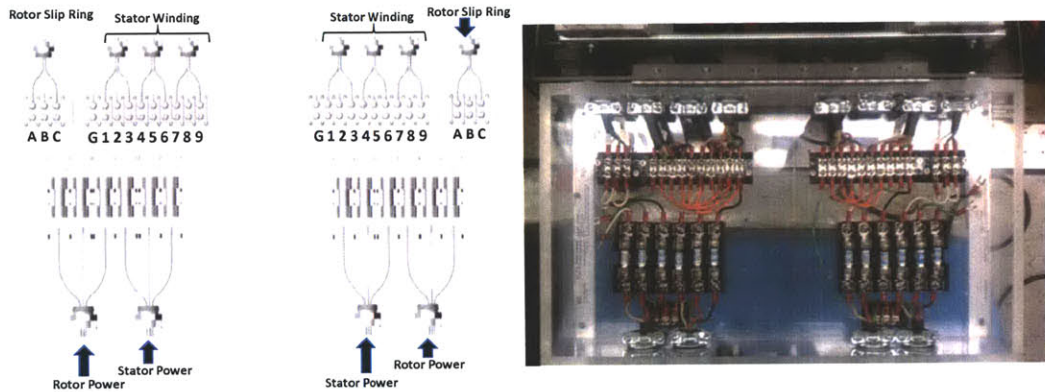


#### Initial Conditions:

1. Inspect all cabling to verify integrity. Ensure that all conductors are intact and that there is no chaffing, a break or damage to the insulation and/or current carrying conductors. In addition verify the following electrical connections to power supplies and to the generator are sufficiently taught (not too tight not too loose):
  - a. DFM supply Cable
  - b. VFD Supply and power cables
  - c. Junction box supply cables
2. Verify wiring in junction box for desired voltage configuration. (Additional wiring diagram supplied in Appendix D)

(This Page Intentionally Left Blank)

Voltage	L1	L2	L3	Join Leads
LOW (230V)	1,7	2,8	3,9	4&5&6
HIGH (460V)	1	2	3	4&7, 5&8, 6&9

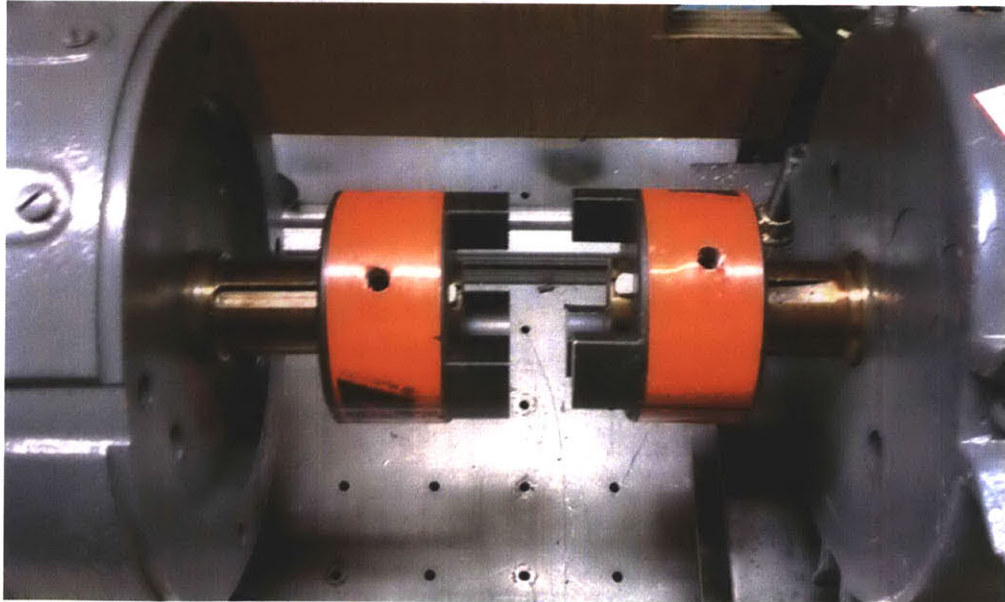


3. Verify the cart placed on level flooring in a low traffic area.
4. Verify the motors rotate freely by hand.
5. Verify motor couplings.
  - a. If operating in a multi-motor setup, verify the coupling between the motors. Inspect the shaft coupling between the motors ensuring that the set screws are tight and that each spider coupling is making sufficient contact with the spider. There should be less than 1/8<sup>th</sup> inch between the coupling hub and the spider. You should not be able to see light through the spider coupling from the opposite side. If coupling is outside of specification, loosen the holding straps and adjust motor until within spec.

(This Page Intentionally Left Blank)



- b. If single motor operation is desired ensure that there is sufficient clearance between the motor couplings or completely remove coupling to prevent damage to the shaft.



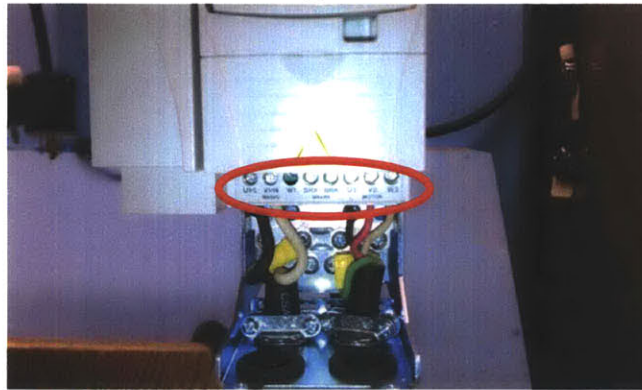
- 6. Verify that the VFD cooling fans are free from debris.

(This Page Intentionally Left Blank)





7. Verify electrical connections to VFD are tight.



### Operating Setup

1. Supply power to the VFD and verify operation
  - a. AC Supply
    - i. If powering VFD from an AC source is desired, connect single phase 200-240 V ac across the U1/L and V1/N terminals.
  - b. DC Supply
    - i. If powering VFD from a DC source is desired, connect 270-325 DC voltage across the BRK- and BRK+ terminal for optimum performance. The VFD DC voltage limit band is 210-420.
2. Once the VFD is powered on, configure the VFD to the specifications of the machine that will be powered using the motor assistant option (*see ABB ACS manual for details*).
3. Connect the VFD output supply to the either the rotor or stator of the DFM.
4. Conduct required experiments

(This Page Intentionally Left Blank)

## APPENDIX C

### MVDC Board MATLAB Code

```
function varargout = DC_zeds_gui(varargin)
%DC_ZEDS_GUI M-file for DC_zeds_gui.fig
%   DC_ZEDS_GUI, by itself, creates a new DC_ZEDS_GUI or raises the existing
%   singleton*.
%
%   H = DC_ZEDS_GUI returns the handle to a new DC_ZEDS_GUI or the handle to
%   the existing singleton*.
%
%   DC_ZEDS_GUI('Property','Value',...) creates a new DC_ZEDS_GUI using the
%   given property value pairs. Unrecognized properties are passed via
%   varargin to DC_zeds_gui_OpeningFcn. This calling syntax produces a
%   warning when there is an existing singleton*.
%
%   DC_ZEDS_GUI('CALLBACK') and DC_ZEDS_GUI('CALLBACK',hObject,...) call the
%   local function named CALLBACK in DC_ZEDS_GUI.M with the given input
%   arguments.
%
%   *See GUI Options on GUIDE's Tools menu. Choose "GUI allows only one
%   instance to run (singleton)".
%
% See also: GUIDE, GUIDATA, GUIHANDLES

% Edit the above text to modify the response to help DC_zeds_gui

% Last Modified by GUIDE v2.5 09-Nov-2010 16:35:45

% Begin initialization code - DO NOT EDIT
gui_Singleton = 1;
gui_State = struct('gui_Name',    mfilename, ...
                  'gui_Singleton', gui_Singleton, ...
                  'gui_OpeningFcn', @DC_zeds_gui_OpeningFcn, ...
                  'gui_OutputFcn', @DC_zeds_gui_OutputFcn, ...
                  'gui_LayoutFcn', [], ...
                  'gui_Callback', []);
if nargin && ischar(varargin{1})
    gui_State.gui_Callback = str2func(varargin{1});
end
```

```

if nargout
    [varargout{1:nargout}] = gui_mainfcn(gui_State, varargin{:});
else
    gui_mainfcn(gui_State, varargin{:});
end
% End initialization code - DO NOT EDIT
end

% --- Executes just before DC_zeds_gui is made visible.
function DC_zeds_gui_OpeningFcn(hObject, eventdata, handles, varargin)
% This function has no output args, see OutputFcn.
% hObject    handle to figure
% eventdata  reserved - to be defined in a future version of MATLAB
% handles    structure with handles and user data (see GUIDATA)
% varargin   unrecognized PropertyName/PropertyValue pairs from the
%           command line (see VARARGIN)

% Choose default command line output for DC_zeds_gui
handles.output = hObject;

% Update handles structure
guidata(hObject, handles);

% UIWAIT makes DC_zeds_gui wait for user response (see UIRESUME)
% uiwait(handles.figure1);
end

% --- Outputs from this function are returned to the command line.
function varargout = DC_zeds_gui_OutputFcn(hObject, eventdata, handles)
% varargout  cell array for returning output args (see VARARGOUT);
% hObject    handle to figure
% eventdata  reserved - to be defined in a future version of MATLAB
% handles    structure with handles and user data (see GUIDATA)

% Get default command line output from handles structure
varargout{1} = handles.output;
end

% Written by Jim Paris at MIT 4/23/2010
function pic_send(s, data)
    if (mod(length(data), 4) ~= 0)
        error('length of data must be a multiple of 4!');
    end
end

```

```

end
for i = 1 : 4 : length(data)
    if (i < length(data) - 4)
        command = '0001'; % write, but don't latch
    else
        command = '0101'; % write and latch
    end
    val = bin2dec([command char(data(i:i+3)+'0')]);
    %fprintf(1, 'writing 0x%02x\n', val);
    fwrite(s, val);
end
end

```

```

% --- Executes on button press in pushbutton1.
function pushbutton1_Callback(hObject, eventdata, handles)
% hObject    handle to pushbutton1 (see GCBO)
% eventdata  reserved - to be defined in a future version of MATLAB
% handles    structure with handles and user data (see GUIDATA)
    global s status;
    status(1:8)=0;
    pic_send(s,status);

    set(handles.togglebutton1,'Value',0);
    set(handles.togglebutton1a,'Value',0);
    set(handles.togglebutton1b,'Value',0);
    set(handles.togglebutton1c,'Value',0);
    set(handles.togglebutton3,'Value',0);
    set(handles.togglebutton3a,'Value',0);
    set(handles.togglebutton3b,'Value',0);
    set(handles.togglebutton3c,'Value',0);

    updateGUI(handles);
end

```

```

% --- Executes on button press in pushbutton2.
function pushbutton2_Callback(hObject, eventdata, handles)
% hObject    handle to pushbutton2 (see GCBO)
% eventdata  reserved - to be defined in a future version of MATLAB
% handles    structure with handles and user data (see GUIDATA)

```

```

% STATUS LOOK-UP TABLE
% 1 : AC2DC1
% 2 : XT1B
% 3 : XT2B
% 4 : XT3B
% 5 : AC2DC3
% 6 : XT1A
% 7 : XT2A
% 8 : XT3A
%

```

```

global s status;
status=zeros(1,8);
set(handles.togglebutton1,'Value',0);
set(handles.togglebutton1a,'Value',0);
set(handles.togglebutton1b,'Value',0);
set(handles.togglebutton1c,'Value',0);
set(handles.togglebutton3,'Value',0);
set(handles.togglebutton3a,'Value',0);
set(handles.togglebutton3b,'Value',0);
set(handles.togglebutton3c,'Value',0);

```

```

s=pic_open('COM3');

```

```

pic_send(s,status);
updateGUI(handles);

```

```

end

```

```

% --- Executes on button press in pushbutton3.

```

```

function pushbutton3_Callback(hObject, eventdata, handles)

```

```

% hObject handle to pushbutton3 (see GCBO)

```

```

% eventdata reserved - to be defined in a future version of MATLAB

```

```

% handles structure with handles and user data (see GUIDATA)

```

```

global s status;
status(1:8)=0;
pic_send(s,status);

```

```

set(handles.togglebutton1,'Value',0);

```

```

set(handles.togglebutton1a,'Value',0);
set(handles.togglebutton1b,'Value',0);
set(handles.togglebutton1c,'Value',0);
set(handles.togglebutton3,'Value',0);
set(handles.togglebutton3a,'Value',0);
set(handles.togglebutton3b,'Value',0);
set(handles.togglebutton3c,'Value',0);

opened = instrfind('Port','COM3');
fclose(opened);

updateGUI(handles);
end

% --- Executes on button press in togglebutton1.
function togglebutton1_Callback(hObject, eventdata, handles)
% hObject    handle to togglebutton1 (see GCBO)
% eventdata  reserved - to be defined in a future version of MATLAB
% handles    structure with handles and user data (see GUIDATA)

% Hint: get(hObject,'Value') returns toggle state of togglebutton1
global s status;
button_state = get(hObject,'Value');

if button_state == get(hObject,'Max')
    % Toggle button is pressed, take appropriate action
    status(1)=1;
    pic_send(s,status);
elseif button_state == get(hObject,'Min')
    % Toggle button is not pressed, take appropriate action
    status(1)=0;
    pic_send(s,status);
end
updateGUI(handles);
end

% --- Executes on button press in togglebutton1a.
function togglebutton1a_Callback(hObject, eventdata, handles)
% hObject    handle to togglebutton1a (see GCBO)
% eventdata  reserved - to be defined in a future version of MATLAB
% handles    structure with handles and user data (see GUIDATA)

```

```
% Hint: get(hObject,'Value') returns toggle state of togglebutton1a
global s status;
button_state = get(hObject,'Value');
```

```
if button_state == get(hObject,'Max')
    % Toggle button is pressed, take appropriate action
    status(2)=1;
    pic_send(s,status);
elseif button_state == get(hObject,'Min')
    % Toggle button is not pressed, take appropriate action
    status(2)=0;
    pic_send(s,status);
end
updateGUI(handles);
```

```
end
```

```
% --- Executes on button press in togglebutton1b.
```

```
function togglebutton1b_Callback(hObject, eventdata, handles)
% hObject handle to togglebutton1b (see GCBO)
% eventdata reserved - to be defined in a future version of MATLAB
% handles structure with handles and user data (see GUIDATA)
```

```
% Hint: get(hObject,'Value') returns toggle state of togglebutton1b
global s status;
button_state = get(hObject,'Value');
```

```
if button_state == get(hObject,'Max')
    % Toggle button is pressed, take appropriate action
    status(3)=1;
    pic_send(s,status);
elseif button_state == get(hObject,'Min')
    % Toggle button is not pressed, take appropriate action
    status(3)=0;
    pic_send(s,status);
end
updateGUI(handles);
```

```
end
```

```
% --- Executes on button press in togglebutton1c.
```

```
function togglebutton1c_Callback(hObject, eventdata, handles)
% hObject handle to togglebutton1c (see GCBO)
% eventdata reserved - to be defined in a future version of MATLAB
```



```

% handles  structure with handles and user data (see GUIDATA)

% Hint: get(hObject,'Value') returns toggle state of togglebutton1c
global s status;
button_state = get(hObject,'Value');

if button_state == get(hObject,'Max')
    % Toggle button is pressed, take appropriate action
    status(4)=1;
    pic_send(s,status);
elseif button_state == get(hObject,'Min')
    % Toggle button is not pressed, take appropriate action
    status(4)=0;
    pic_send(s,status);
end
updateGUI(handles);
end

```

```

% --- Executes on button press in togglebutton3.
function togglebutton3_Callback(hObject, eventdata, handles)
% hObject  handle to togglebutton3 (see GCBO)
% eventdata reserved - to be defined in a future version of MATLAB
% handles  structure with handles and user data (see GUIDATA)

```

```

% Hint: get(hObject,'Value') returns toggle state of togglebutton3
global s status;
button_state = get(hObject,'Value');

if button_state == get(hObject,'Max')
    % Toggle button is pressed, take appropriate action
    status(5)=1;
    pic_send(s,status);
elseif button_state == get(hObject,'Min')
    % Toggle button is not pressed, take appropriate action
    status(5)=0;
    pic_send(s,status);
end
updateGUI(handles);
end

```

```

% --- Executes on button press in togglebutton3a.
function togglebutton3a_Callback(hObject, eventdata, handles)

```

```

% hObject handle to togglebutton3a (see GCBO)
% eventdata reserved - to be defined in a future version of MATLAB
% handles structure with handles and user data (see GUIDATA)

% Hint: get(hObject,'Value') returns toggle state of togglebutton3a
global s status;
button_state = get(hObject,'Value');

if button_state == get(hObject,'Max')
    % Toggle button is pressed, take appropriate action
    status(6)=1;
    pic_send(s,status);
elseif button_state == get(hObject,'Min')
    % Toggle button is not pressed, take appropriate action
    status(6)=0;
    pic_send(s,status);
end
updateGUI(handles);
end

```

```

% --- Executes on button press in togglebutton3b.
function togglebutton3b_Callback(hObject, eventdata, handles)
% hObject handle to togglebutton3b (see GCBO)
% eventdata reserved - to be defined in a future version of MATLAB
% handles structure with handles and user data (see GUIDATA)

% Hint: get(hObject,'Value') returns toggle state of togglebutton3b
global s status;
button_state = get(hObject,'Value');

if button_state == get(hObject,'Max')
    % Toggle button is pressed, take appropriate action
    status(7)=1;
    pic_send(s,status);
elseif button_state == get(hObject,'Min')
    % Toggle button is not pressed, take appropriate action
    status(7)=0;
    pic_send(s,status);
end
updateGUI(handles);
end

```

```

% --- Executes on button press in togglebutton3c.
function togglebutton3c_Callback(hObject, eventdata, handles)
% hObject    handle to togglebutton3c (see GCBO)
% eventdata  reserved - to be defined in a future version of MATLAB
% handles    structure with handles and user data (see GUIDATA)

% Hint: get(hObject,'Value') returns toggle state of togglebutton3c
global s status;
button_state = get(hObject,'Value');

if button_state == get(hObject,'Max')
    % Toggle button is pressed, take appropriate action
    status(8)=1;
    pic_send(s,status);
elseif button_state == get(hObject,'Min')
    % Toggle button is not pressed, take appropriate action
    status(8)=0;
    pic_send(s,status);
end
updateGUI(handles);
end

function updateGUI(handles)
% STATUS LOOK-UP TABLE
% 1 : AC2DC1
% 2 : XT1B
% 3 : XT2B
% 4 : XT3B
% 5 : AC2DC3
% 6 : XT1A
% 7 : XT2A
% 8 : XT3A

global status;
AC2DC1 = status(1);
XT1B = status(2);
XT2B = status(3);
XT3B = status(4);
AC2DC3 = status(5);
XT1A = status(6);
XT2A = status(7);
XT3A = status(8);

```

```

nodecolor = zeros(size(status));

if(AC2DC1)
    nodecolor(1) = 1;
    nodecolor(2) = XT1B;
    nodecolor(3) = XT2B;
    nodecolor(4) = XT3B;
end

if(AC2DC3)
    nodecolor(5) = 1;
    nodecolor(6) = XT1A;
    nodecolor(7) = XT2A;
    nodecolor(8) = XT3A;
end
texts = { {'1','1a','1b','1c'},...
          {'11b'},...
          {'12b'},...
          {'13b'},...
          {'3','3a','3b','3c'},...
          {'31a'},...
          {'32a'},...
          {'33a'},...
          };

for k=1:length(status)
    num = floor(k/5);
    if(nodecolor(k)==1)
        color = [1-num 0 num];
    else
        color = [1 1 1];
    end
    text = texts{k};
    for m=1:length(text)
        eval(strcat(['tb = handles.text',text{m},'],'));
        set(tb,'BackgroundColor',color);
    end
end

end

end

```

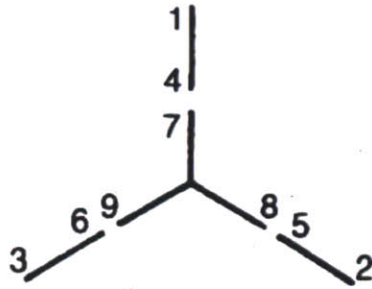
## APPENDIX D

### DFM Wiring Schematic

#### TERMINAL MARKINGS AND CONNECTIONS FOR SINGLE-SPEED, THREE-PHASE MOTORS—9 LEADS

---

---



#### DUAL VOLTAGE Y-CONNECTED

VOLTAGE	L1	L2	L3	JOIN
LOW	1,7	2,8	3,9	4&5&6
HIGH	1	2	3	4&7,5&8,6&9

(This Page Intentionally Left Blank)

## **APPENDIX E**

Points of Contact

### **Hitachi VFD Tech Support**

**Paul Curtis**

**Paul.Curtis@hal.hitachi.com**

*Assistant Product Manager*

*AC Inverter Products*

Hitachi America, Ltd.

Tarrytown, NY

914-524-6663

**Chris Elley**

**christopher.elley@hal.hitachi.com**

*Sr. Distribution Sales Specialist*

*AC Inverters*

Hitachi America Ltd.

4731 NW Cliff Hill Circle

Kansas City, MO 64151

Cell: 816-803-9493

Fax: 816-587-1578

### **ABB VFD Tech Support**

**Todd Vigorito**

**todd.vigorito@tulimieri.com**

Cell: 860-918-2758

### **VFD Retailers**

**Kelly York**

**kelly@ics-limited.com**

**Industrial Control Specialists Ltd**

8 Delta Drive

Londonderry, NH

(800) 370-2283

(603) 625-2900

### **Doubly-fed Machine Tech Support and Retailer**

**Doug Beat**

**dougbeat@dougbeat.com**

Phone 419-841-3881